Dynamics of shape fluctuations of quasi-spherical vesicles revisited

Ling Miao[a], Michael A. Lomholt[b], and Jesper Kleis

The MEMPHYS Center for Biomembrane Physics, Physics Department, University of Southern Denmark, DK-5230 Odense M, Denmark

Abstract. In this paper, the dynamics of spontaneous shape fluctuations of a single, giant quasi-spherical vesicle formed of a single lipid species is revisited theoretically. A coherent physical theory for the dynamics is developed based on a number of fundamental principles and considerations and a systematic formulation of the theory is also established. From the systematic theoretical formulation, an analytical description of the dynamics of shape fluctuations of quasi-spherical vesicles is derived. In particular, in developing the theory we have made a new interpretation of some of the phenomenological constants in a canonical continuum description of fluid lipid-bilayer membranes and shown the consequences of this new interpretation in terms of the characteristics of the dynamics of vesicle shape fluctuations. Moreover, we have used the systematic formulation of our theory as a framework against which we have discussed the previously existing theories and their discrepancies. Finally, we have made a systematic prediction about the system-dependent characteristics of the relaxation dynamics of shape fluctuations of quasi-spherical vesicles with a view of experimental studies of the phenomenon and also discussed, based on our theory, a recently published experimental work on the topic.

PACS. 68.15.+e Liquid thin films. – 87.16.Dg Membranes, bilayers, and vesicles.

1 Introduction

Dynamics of fluid membranes was already observed a couple of centuries ago, as "flickering" seen under optical microscope of resting red blood cells. The first physical study of the "flickering" phenomenon of red blood cells was made, however, only in 1975 by Brochard and Lennon [1]. They presented the first theory for the phenomenon, where they employed the concept of bending elasticity due to Helfrich [2] for describing the conformational flexibility of fluid membranes and associated the "flickering" with the dynamics of equilibrium shape fluctuations of red-cell membranes that are thermally driven due to the conformational flexibility of the membranes. This association has since become one of the essential ideas in theories for dynamics of fluid membranes.

During the last three decades, unilamellar lipid-bilayer vesicles reaching micrometer sizes that can be routinely prepared in the laboratory have provided one of the most important classes of model systems for biological cell membranes. They allow for well-defined and quantitative physical investigations of the conformational behaviour of fluid membranes. The relevant physics governing the *static* equilibrium shapes of giant, unilamellar vesicles has been fully understood, as the result of a series of both theoretical and experimental studies [3,4,5,6]. The static properties of equilibrium shape fluctuations have also been investigated [7,8,9]. The understanding of the dynamics of equilibrium shape fluctuations of the vesicles has not, however, reached the same stage. This is largely the consequence of the fact that the dynamics of fluid membranes involves many more physical factors than the statics. The static properties of a fluid membrane in thermodynamic equilibrium are entirely determined by thermodynamic energetics of the membrane alone. In contrast, the dynamics of the membrane is not only related to the thermodynamic energetics, but also depends on the dynamics of the bulk aqueous fluid in which the membrane is suspended: motion of the membrane induces motion in the bulk fluid, which in turn exerts hydrodynamic force on the membrane. Furthermore, any intrinsic dissipation mechanisms of the membrane will in principle play a role in the dynamics.

Many studies, both experimental and theoretical, have actually focused on the dynamics of fluid membranes. The earlier work of Schneider *et al.* [10] investigated experimentally by use of fluorescence microscopy the fluctuation spectrum of giant, unilamellar and quasi-spherical vesicles. In the theoretical interpretation of the experimental data, Schneider *et al.*, and later, Milner and Safran [7], treated the energetics of the membrane as that of a *single* and *incompressible* fluid surface with the Helfrich bending rigidity. Moreover, they neglected any intrinsic dissipation

[a] *e-mail:* miao@fysik.sdu.dk
[b] *e-mail:* mlomholt@fysik.sdu.dk

of the membrane. Their theory predicted a single relaxation rate for each spherical-harmonic mode of the vesicle shape fluctuations.

The earlier notion that a lipid-bilayer membrane could be considered as a single and incompressible fluid surface soon had to be modified. The relevance of both the *bilayer* architecture of the membrane and the *compressibility* of the constituting monolayers was first appreciated and demonstrated in the context of equilibrium shapes of giant lipid-bilayer vesicles [5,6,11,12,13]. Evans and Yeung soon also pointed out the relevance of this new notion to the conformational dynamics of giant vesicles [14]. Based on their analysis of a tether-pulling experiment on giant vesicles, they proposed that the bilayer structure of the membrane in fact allows the two monolayers to move relative to each other laterally and that the relative motion is associated with dissipation of energy phenomenologically described as *intermonolayer friction*. Moreover, they suggested a coupling between bending of the membrane and a local field of relative area dilation/compression of the monolayers, whose relaxation in turn drives the relative intermonolayer motion. In this theory, therefore, the conformational dynamics of a fluid membrane would be coupled to dynamics of the relative monolayer dilation/compression field.

Following the idea put forward by Evans and Yeung [14], Seifert and Langer formulated a theoretical description of the paradigmatic case of the dynamics of equilibrium fluctuations of an almost planar bilayer membrane embedded in a viscous aqueous medium [15]. They also discussed the relevance of their result to the experimental measurements made by spin-echo technique on multilamellar membrane stacks. No conclusive confirmation of the theory, however, could be made due to the lack of direct experimental data.

Giant, quasi-spherical vesicles, whose fluctuations can be observed directly by video microscopy, provide another type of systems, for which a theory for the dynamics can in principle be put to a quantitative test against experimental data. Yeung and Evans [16], and later, Bivas *et al.* [17], considered such systems. Each group presented a theoretical formulation of its own for the dynamics of equilibrium fluctuations of quasi-spherical vesicles. Although, qualitatively speaking, the two theories were similar in that both used the ideas originally proposed by Evans and Yeung [14], they differed both in their detailed descriptions of the thermodynamic energetics of the vesicles and in their formulations of the equations of motion. Consequently, the two theories yielded different analytical results that characterize the dynamics. It is, however, not straightforward to justify either of the two theories. Yeung and Evans employed a description of the thermodynamic free energy of the vesicle membrane, that would be consistent with the assumption that local density inhomogeneities in the monolayers relaxed much faster than bending deformations. But the assumption is inconsistent with the basic starting point of their theory, which was to treat the dynamics of bending and density inhomogeneities on the same footing. Bivas *et al.*, while proposing and using a phenomenological model for the thermodynamic free energy that was consistent with their considerations of dynamics, adopted an *ad hoc* approach to the formulation of equations of motion that ultimately governed the dynamics. The approach lacks the rigor that a systematic approach based on some fundamental principles would otherwise have. Its justification is, therefore, less than transparent. Moreover, a number of approximations were used in both theories, for which the justifications were not clear either, due to the absence of a systematic formalism. It is thus our opinion that a physically consistent and systematic theory for the dynamics of equilibrium fluctuations of quasi-spherical vesicles is still needed.

Continuing experiments on giant, quasi-spherical vesicles by the use of phase contrast video microscopy further underline the need for a well-defined theory. A recent analysis [18] of the experimental data obtained by the use of the techniques indicates that the dynamics of equilibrium fluctuations of giant vesicles involves more relaxation processes than the single process of relaxation of bending predicted by the theory of Schneider *et al.* [10] and Milner and Safran [7]. The still improving time resolution of the video-microscopy technique will also lead to a large amount of experimental data of better quality. Having a systematic and well-defined theory will greatly facilitate the analysis and interpretation of the experimental data as well as the quantitative test of the theory itself, thus furthering our understanding of the phenomenon.

The purpose of this paper is, therefore, two-fold. First, we will present, based on a number of fundamental principles and considerations, a coherent physical theory, and a systematic formulation of the theory for the dynamics of equilibrium fluctuations of giant, quasi-spherical vesicles formed of a single lipid species. One fundamental consideration underlying the theory is Onsager's regression hypothesis: the average regression of the spontaneous thermal fluctuations in a macroscopic system obeys the sames laws as the corresponding macroscopic irreversible processes [19]. Following this hypothesis, we may understand the dynamics of the thermal fluctuations in a giant vesicle by investigating the near-equilibrium dynamics of the same system. Our starting point for formulating the near-equilibrium dynamics of a giant vesicle is then to describe the vesicle dynamics as the hydrodynamics of two coupled systems of (quasi-)two-dimensional fluid with time-dependent surface geometry. This description of the surface hydrodynamics of the membrane thus naturally involves both a thermodynamic description of the membrane and a description of the hydrodynamics of the bulk fluids surrounding the vesicle from within and without. Formulated this way, the theory, including the various approximations that will be made, appears conceptually transparent and systematic. This feature not only will make the comparison between the theory and the experiments, and in turn, any necessary modifications easier, but will also lend the formalism readily to any extension that deals with vesicle systems of more complexity, for example, giant vesicles made either of two lipid species or of a lipid species with a membrane protein species. Sec-

ondly, we will present, as an application of the general formalism, a specific derivation of analytical expressions for the regression dynamics of shape fluctuations of quasi-spherical vesicles. In particular we discuss systematically the different approximations employed in the application. Our results are different from those derived by Yeung and Evans [16] and by Bivas *et al.* [17], and we will discuss the differences. To facilitate the comparison of the theory with the experiments, we also present a systematic numerical analysis of the analytical results.

The plan of the presentation is as follows. In Section 2, we introduce and discuss a thermodynamic description of fluid lipid-bilayer membranes. In Section 3, we present a systematic formulation of near-equilibrium dynamics of fluid-bilayer vesicles, which can in principle be applied to vesicles with arbitrary equilibrium shapes. In Section 4, we apply the general formulation described in Section 3 to systems of quasi-spherical vesicles. Finally, in Section 5, we discuss the implications that our results have for experimental measurements on the dynamics of spontaneous shape fluctuations of quasi-spherical vesicles. We will also discuss the differences and connections between our results and the theoretical results obtained by other groups previously [16,17].

2 Thermodynamic description of fluid lipid-bilayer membranes

In this section, we will consider a vesicle formed of a closed fluid lipid-bilayer membrane containing only a single lipid species. The vesicle encloses a volume of V, which can be considered fixed under typical experimental conditions. The two constituting monolayers of the vesicle membrane, the outer one labeled by superscript "+" and the inner one by "−", contain N^+ and N^- lipid molecules, respectively. As has been recognized [5], N^+ and N^- depend on the vesicle formation process and may be different from each other. A total area, $A_{\rm m}$, that can be resolved with techniques of microscopic resolutions or with equivalent means, can be defined for the whole membrane. To a good approximation, $A_{\rm m}$ may be treated, for most of the membrane systems studied, as a fixed quantity that depends on N^+ and N^-. When a vesicle is flaccid, in other words, having a non-zero excess area $\Delta \equiv A_{\rm m}/4\pi R_{\rm v}^2 - 1$, where $R_{\rm v} \equiv (3V/4\pi)^{1/3}$, it undergoes thermally driven conformational fluctuations as a result of the membrane flexibility. In the case of giant vesicles that are typically investigated, whose sizes are in the micrometer range and whose bending rigidities are of the order of 10^{-19} J, the fluctuations remain controlled. Thus, the vesicle we consider has a well-defined equilibrium shape, whose specific geometry depends on V, N^+, N^- and temperature T.

We will present a phenomenological description of the thermodynamics of a fluid lipid-bilayer membrane, which is consistent with our starting point that the membrane is conformationally flexible and consists of two weakly coupled compressible monolayers. This description will form a necessary part of the formulation of the membrane dynamics.

2.1 Notations and relevant fields

To describe the conformational flexibility of a fluid membrane, we use the basic notation of surface differential geometry. At length scales larger than molecular lengths, the varying conformation of a fluid membrane suspended in a bulk aqueous fluid can be approximated by a two-dimensional surface embedded in the three-dimensional space and with a time-dependent geometry. Such a surface can be represented by a three-dimensional vector, $\boldsymbol{R}(u^1, u^2, t)$, where u^1 and u^2 are the two coordinates parametrizing the two-dimensional internal space and t represents time. The derivatives of $\boldsymbol{R}(u^1, u^2, t)$ with respect to the internal coordinates u^α ($\alpha = 1, 2$) define two local tangent vectors to the surface:

$$\boldsymbol{t}_\alpha(u^1, u^2, t) \equiv \frac{\partial \boldsymbol{R}(u^1, u^2, t)}{\partial u^\alpha} \equiv \partial_\alpha \boldsymbol{R}(u^1, u^2, t), \quad \alpha = 1, 2. \tag{1}$$

From $\boldsymbol{t}_1$ and $\boldsymbol{t}_2$, a local unit vector normal to the surface can be constructed:

$$\boldsymbol{n} \equiv \frac{\boldsymbol{t}_1 \times \boldsymbol{t}_2}{|\boldsymbol{t}_1 \times \boldsymbol{t}_2|} \, . \tag{2}$$

The metric tensor $a_{\alpha\beta}$ of the surface is then given by

$$a_{\alpha\beta} = \boldsymbol{t}_\alpha \cdot \boldsymbol{t}_\beta \, , \tag{3}$$

which is a symmetric tensor with a non-zero determinant $a \equiv \det(a_{\alpha\beta})$. A local area element, dA, can be expressed as

$$dA = \sqrt{a}\, du^1 du^2. \tag{4}$$

The inverse of the metric tensor, $a^{\alpha\beta}$, follows from

$$a^{\alpha\beta} a_{\beta\gamma} = \delta^\alpha_\gamma \, , \tag{5}$$

leading to the definitions of contravariant surface tangent vectors $\boldsymbol{t}^\alpha \equiv a^{\alpha\beta}\boldsymbol{t}_\beta$. The rule of summation over repeated Greek indices has been used in the above expressions, and will be kept to in the rest of the paper. Clearly, $\boldsymbol{t}^\alpha \cdot \boldsymbol{t}_\beta = \delta^\alpha_\beta$. Any space vector $\boldsymbol{w}$ tangent to the surface can be expressed as $\boldsymbol{w} = w_\alpha \boldsymbol{t}^\alpha = w^\alpha \boldsymbol{t}_\alpha$, where $w_\alpha = \boldsymbol{w} \cdot \boldsymbol{t}_\alpha$ and $w^\alpha = \boldsymbol{w} \cdot \boldsymbol{t}^\alpha = a^{\alpha\beta} w_\beta$ are the covariant and contravariant components of $\boldsymbol{w}$, respectively.

A full description of the essential local properties of the surface requires also the information contained in

$$\partial_\alpha \partial_\beta \boldsymbol{R} = \Gamma^\gamma_{\alpha\beta} \partial_\gamma \boldsymbol{R} + b_{\alpha\beta} \boldsymbol{n} \, , \tag{6}$$

where $b_{\alpha\beta} \equiv \boldsymbol{n} \cdot \partial_\alpha \partial_\beta \boldsymbol{R}$ is the so-called "curvature tensor", and $\Gamma^\gamma_{\alpha\beta}$ defines the Christoffel symbol. From the curvature tensor both the mean curvature H and the Gaussian curvature K can be obtained, respectively,

$$H \equiv \frac{1}{2} a^{\alpha\beta} b_{\alpha\beta} = \frac{1}{2} \left(\frac{1}{R_1} + \frac{1}{R_2} \right) \, , \tag{7}$$

and

$$K \equiv \det\left(a^{\alpha\gamma} b_{\gamma\beta}\right) = \frac{1}{R_1} \cdot \frac{1}{R_2} \tag{8}$$

where R_1 and R_2 are the two principal radii of curvature.

By use of the Christoffel symbol $\Gamma^{\gamma}_{\alpha\beta}$, covariant differentiations with respect to u^{α}, denoted by D_{α}, of surface scalars, vectors and tensors can be performed. For any surface scalar, $\rho(u^1,u^2)$, $D_{\alpha}\rho(u^1,u^2)=\partial_{\alpha}\rho(u^1,u^2)$, and for a surface vector represented by its contravariant components, w^{α}, $D_{\alpha}w^{\gamma}=\partial_{\alpha}w^{\gamma}+\Gamma^{\gamma}_{\alpha\beta}w^{\beta}$.

In order to fully characterize the physical state of a flexible and compressible fluid lipid-bilayer membrane formed of a single lipid species, two more fields are needed in addition to $\boldsymbol{R}(u^1,u^2,t)$: $\rho^+(u^1,u^2,t)$ and $\rho^-(u^1,u^2,t)$, representing the local surface (number) densities of the outer and inner monolayer, respectively, and defined with respect to the surface described by $\boldsymbol{R}(u^1,u^2,t)$.

2.2 Thermodynamic free energy

Imagine a vesicle suspended in a bulk fluid at temperature T. Its equilibrium (relaxed) state is then characterized both by an average shape $\boldsymbol{R}_0(u^1,u^2)$ and by average monolayer densities $\rho_0^+(u^1,u^2)\equiv N^+/A_0$ and $\rho_0^-(u^1,u^2)\equiv N^-/A_0$ [1], where A_0 is the area defined by the average shape. For later use, we define

$$N_{\Sigma}\equiv\frac{N^++N^-}{2}\ ,\quad N_{\Delta}\equiv\frac{N^+-N^-}{2}\ .$$

Assume now that the vesicle is in a near-equilibrium state with an effective shape described by $\boldsymbol{R}(u^1,u^2,t)$ and with density fields $\rho^+(u^1,u^2,t)$ and $\rho^-(u^1,u^2,t)$ describing respective inhomogeneities in the two monolayers. We associate the following thermodynamic free energy to the near-equilibrium state of the vesicle:

$$\begin{aligned}F=&\int dA\ \frac{k_{\rm eff}}{2}\ \left(\frac{\rho^+}{\rho_0}-1\right)^2+\int dA\ \frac{k_{\rm eff}}{2}\ \left(\frac{\rho^-}{\rho_0}-1\right)^2\\&+\int dA\ \gamma(\rho^+-\rho_0)+\int dA\ \gamma(\rho^--\rho_0)+\sigma\int dA\\&+\int dA\ \frac{\kappa_{\rm eff}}{2}(2H)^2+\int dA\ \lambda H(\frac{\rho^+}{\rho_0}-\frac{\rho^-}{\rho_0})\ .\end{aligned}\tag{9}$$

The five terms in the first two lines may be viewed as the result of an expansion of a local free energy function, $F_{T,\Delta}(N^+_{\Delta},N^-_{\Delta},A_{\Delta})=A_{\Delta}f(T,\rho^+,\rho^-)$, about a particular reference value, ρ_0, of the monolayer surface densities. In other words, the first four terms describe the free-energy cost associated with deviations in the monolayer surface densities from the reference value and the last of the five terms represents the free energy required to change the area of the effective shape of the vesicle at constant density, ρ_0. Consequently, the constant parameters, $k_{\rm eff}$, γ, and σ, all depend on the chosen reference state. $k_{\rm eff}$, in particular, is the monolayer compressibility modulus corresponding to the chosen ρ_0. The first term in the last line of Eq.(9) represents the free-energy cost associated with bending of the membrane, and the second term takes into account a possible coupling between the bending of the membrane and the difference between local monolayer surface densities: a non-zero $(\rho^+-\rho^-)$ may be viewed as amounting to a dynamic spontaneous curvature [15,20,21].

Eq.(9) can be rewritten as

$$\begin{aligned}F=&\int dA\ \frac{k_{\rm eff}}{2}\ \left(\frac{\rho^+}{\rho_0}-1\right)^2+\int dA\ \frac{k_{\rm eff}}{2}\ \left(\frac{\rho^-}{\rho_0}-1\right)^2\\&+\int dA\ \gamma\rho^++\int dA\ \gamma\rho^-+\int dA\ \frac{\kappa_{\rm eff}}{2}(2H)^2\\&+\int dA\ \lambda H(\frac{\rho^+}{\rho_0}-\frac{\rho^-}{\rho_0})+\sigma_0\int dA\ ,\end{aligned}\tag{10}$$

where $\sigma_0\equiv\sigma-2\gamma\rho_0$. The terms $\int dA\ \gamma\rho^+$ and $\int dA\ \gamma\rho^-$ will be dropped henceforth since we will only consider situations where the number of lipid molecules in each monolayer is conserved.

A couple of important remarks on the physical interpretation of the above free energy are due here. First, since our theory is intended to describe the dynamics of vesicle conformation that can be resolved at optical or *mesoscopic* length scales, the free energy should be understood as an effective Hamiltonian resulted from an appropriate coarse-graining procedure which integrates over fluctuations at suboptical scales [22,23]. The work presented in Refs. [22,23] makes it conceptually clear that the physical parameters describing the elastic properties of the vesicle membrane at the mesoscopic length scales, namely, $k_{\rm eff}$, $\kappa_{\rm eff}$, and λ, are "renormalized" parameters, different in principle from those parameters describing the elastic properties of the membrane at *microscopic* length scales. For the same reason, the constant σ_0 conjugate to the "apparent" membrane area under an optical resolution is an *effective membrane tension* [23], and is distinct both from the microscopic surface tension and from the mechanical frame tension which is associated with the equilibrium shape and which can be accessed by micromechanical measurements [24,25].

This issue has not been addressed before in the previous works on membrane and vesicle dynamics [15,16,17]. And, one might argue that, when fluctuations are sufficiently small to allow a Gaussian (linear) theory of the fluctuations, the distinction between the effective elastic parameters at the mesoscopic length scales and the elastic parameters at microscopic length scales would only be conceptual rather than quantitative, as the conventional wisdom on linear theories of fluctuations may lead one to believe. However, the work reported in Refs. [22,23] clearly shows that care must be taken when we apply the conventional wisdom to fluid membrane systems. In particular, if we consider a vesicle whose membrane is nearly incompressible at microscopic length scales and which is in either a *floppy* state or a *entropic-tense* state [23], the effective area compressibility modulus $k_{\rm eff}$ of the vesicle membrane at mesoscopic length scales originates almost entirely from integrating over small fluctuations at suboptical length scales and is smaller than the microscopic area compressibility modulus. We will show in later discussions

[1] Strictly speaking, $\rho_0^+(u^1,u^2)$ and $\rho_0^-(u^1,u^2)$ may not be constant for non-spherical shapes.

that our new interpretation of the physical parameters in the model free energy bears consequences for the qualitative as well as quantitative characterization of vesicle dynamics.

The second remark concerns the validity of the expansion form of the free energy, and relatedly, the choice of the reference state, represented by ρ_0. As discussed in Ref. [23], the effective free energy associated with optical length scales involves a *nonlinear* area elasticity. Therefore, the expansion, which only contains *linear* area elasticity, is valid in principle only when deviations from the chosen reference state ρ_0 are small. Thus, for our considerations of near-equilibrium states, a natural choice of ρ_0 is

$$\rho_0 = N_\Sigma / A_0 \ , \tag{11}$$

Finally, with definitions $\phi^\pm \equiv \rho^\pm/\rho_0 - 1$, Eq.(10) can be rewritten as

$$\begin{aligned} F = & \int dA \ \frac{k_{\rm eff}}{2}(\phi^+)^2 + \int dA \ \frac{k_{\rm eff}}{2}(\phi^-)^2 \\ & + \int dA \ \frac{\kappa_{\rm eff}}{2}(2H)^2 + \int dA \ \lambda H(\phi^+ - \phi^-) \\ & + \sigma_0 \int dA \ . \end{aligned} \tag{12}$$

3 A systematic and general formulation of vesicle dynamics

In this section, we will present a formulation of vesicle dynamics. The formulation is both systematic, relying on various basic concepts and notions from condensed matter physics, and general, in that it can in principle be applied to vesicles with arbitrary geometry.

3.1 Surface hydrodynamics of the membrane: Equations of motion

Following our discussion of vesicle dynamics in **Introduction**, we begin with a hydrodynamic description of the surface flows within the two fluid monolayers constituting the vesicle membrane. The description treats the two monolayers as two individual, but weakly coupled, systems of quasi-two-dimensional fluids; it also takes into account the fact that each monolayer interacts with its corresponding bulk fluid environment. Moreover, it is assumed in the description that the motions within the two monolayers take place under isothermal conditions, leaving to be considered for each monolayer only two intrinsic hydrodynamic fields, the density field and the surface velocity field. Consequently, the surface hydrodynamics of each monolayer is principally governed by two equations of motion: one states the law of mass (particle) conservation, and the other expresses the generalized law of momentum conservation.

To facilitate the presentation, we first introduce some additional notations related to the dynamics. Let's consider a fluid surface described by $\boldsymbol{R}(u^1, u^2, t)$, and let the trajectory of a particular material particle be represented by $u^\alpha = u^\alpha(\xi, t), \alpha = 1, 2$ where ξ labels the material particle. The covariant components of the intrinsic velocity of the particle are then defined by

$$W^\alpha \equiv \frac{du^\alpha}{dt} \equiv \left.\frac{\partial u^\alpha(\xi,t)}{\partial t}\right|_\xi \ . \tag{13}$$

The material velocity of the particle in the three dimensional embedding space can be obtained easily:

$$\begin{aligned} \boldsymbol{U} \equiv & \left.\frac{d\boldsymbol{R}(u^1,u^2,t)}{dt}\right|_\xi = W^\alpha \boldsymbol{t}_\alpha + \left.\frac{\partial \boldsymbol{R}(u^1,u^2,t)}{\partial t}\right|_u \\ \equiv & W^\alpha \boldsymbol{t}_\alpha + \partial_t \boldsymbol{R} \ . \end{aligned} \tag{14}$$

$\boldsymbol{U}$ may also be expressed as a decomposition into components tangential and normal to the surface,

$$\boldsymbol{U} = \boldsymbol{U}_{\rm t} + U_{\rm n}\boldsymbol{n} \ , \tag{15}$$

where $U_{\rm n} \equiv \boldsymbol{U}\cdot\boldsymbol{n}$ and $\boldsymbol{U}_{\rm t} = U^\alpha \boldsymbol{t}_\alpha$. U^α is in general not equal to W^α as a result of the time-varying geometry, but is related to W^α as follows,

$$U^\alpha = W^\alpha + a^{\alpha\beta}\boldsymbol{t}_\beta \cdot (\partial_t \boldsymbol{R}) \ . \tag{16}$$

For any function $f(u^1, u^2, t)$ defined on the fluid surface, a useful time derivative may be defined:

$$D_t f(u^1,u^2,t) \equiv a^{-1/2}\partial_t(a^{1/2}f) = \partial_t f + f\frac{\partial_t a}{2a} \ . \tag{17}$$

3.1.1 Equations of motion

We can now write down the four principal equations of motion, two for each monolayer, that govern the dynamics of a fluid lipid-bilayer vesicle. The formalistic derivations of the equations are given elsewhere [22,26]. Given the monolayer surface density fields, $\rho^\pm(u^1, u^2, t)$, and the intrinsic velocity fields, $W^\alpha_\pm(u^1, u^2, t)$, we can define intrinsic particle fluxes, $j^\alpha_\pm \equiv \rho^\pm W^\alpha_\pm$. The subscripts "+" and "−", same as the superscripts, refer to the outer and the inner monolayer of the vesicle, respectively. The law of mass (particle) conservation for each monolayer can then be expressed in covariant form as follows,

$$D_t\rho^\pm + D_\alpha j^\alpha_\pm = 0 \ , \tag{18}$$

where D_t and D_α have been defined previously.

The generalized law of momentum conservation can also be written in a similar way. For each monolayer, a three-dimensional vector representing the surface density of monolayer momentum can be defined by $\boldsymbol{J}_\pm \equiv m\rho^\pm\boldsymbol{U}^\pm = m\rho^\pm(W^\alpha_\pm\boldsymbol{t}_\alpha + \partial_t\boldsymbol{R})$, where m is the molecular mass of the constituting lipid. The equations of motion governing the changes of $\boldsymbol{J}_\pm$ take the following form:

$$D_t\boldsymbol{J}_\pm + D_\alpha(j^\alpha_\pm \boldsymbol{J}_\pm) = \boldsymbol{f}^\pm \ , \tag{19}$$

where $j^\alpha_\pm\boldsymbol{J}_\pm$ are the covariant momentum fluxes. $\boldsymbol{f}^\pm$ represent the total forces per unit area acting on the monolayers.

3.2 Forces acting on monolayer surfaces

In principle $\boldsymbol{f}^{\pm}$ should contain several forces of different origins: any dissipative forces associated with the intrinsic surface shear and dilational viscosities of the monolayers; $\boldsymbol{f}^{\pm}_{\rm m}$, forces which the two monolayers exert on each other; $\boldsymbol{f}^{\pm}_{\rm rs}$, the mechanical (restoring) forces associated with the free energy Eq.(12); and, finally, $\boldsymbol{T}^{\pm}$, the hydrodynamic forces exerted on the monolayers by their corresponding bulk fluids. In the following, we discuss each of the four types of forces in turn.

In our theory of vesicle dynamics, we have neglected the intrinsic dissipative forces within each individual monolayer, based on the evidence and arguments given in Ref. [16]. The intermonolayer forces, $\boldsymbol{f}^{\pm}_{\rm m}$, may be modelled as

$$\boldsymbol{f}^{\pm}_{\rm m} = \mp b(\boldsymbol{U}^{+}_{\rm t} - \boldsymbol{U}^{-}_{\rm t}) + \boldsymbol{f}^{\pm}_{\rm n} \,, \tag{20}$$

where

$$\boldsymbol{f}^{\pm}_{\rm b} \equiv \mp b(\boldsymbol{U}^{+}_{\rm t} - \boldsymbol{U}^{-}_{\rm t}) \,, \tag{21}$$

phenomenologically describes dissipation associated with the relative motion between the monolayers. Thus, b may be called the "intermonolayer friction coefficient." This description was originally proposed by Evans *et al.* [14]. $\boldsymbol{f}^{\pm}_{\rm n}$, with $\boldsymbol{f}^{+}_{\rm n} = -\boldsymbol{f}^{-}_{\rm n}$, represent the normal components of the intermonolayer forces, which constrain the motions of the two monolayers in the normal direction.

3.2.1 Mechanical restoring force

In deriving from the free energy given in Eq.(12) the mechanical restoring force acting on each individual monolayer, we may imagine the following infinitesimal virtual variation in the geometry of each monolayer:

$$\boldsymbol{R}(u^1,u^2,t) \to \boldsymbol{R}(u^1,u^2,t) + \delta\boldsymbol{R}(u^1,u^2) \,, \tag{22}$$

and define the restoring forces $\boldsymbol{f}^{\pm}_{\rm rs}$ through

$$\delta F^{\pm} = \oint dA\, (-\boldsymbol{f}^{\pm}_{\rm rs}) \cdot \delta\boldsymbol{R} \,. \tag{23}$$

where δF^{+} and δF^{-} are the variations in the free energies of the two monolayers $F^{\pm}$ induced by the shape variation $\delta\boldsymbol{R}$.

Two issues are implicit in Eq.(23), which need to be addressed clearly. The first is the issue of how to evaluate $F^{\pm}$. This issue has not been discussed at all in the current literature on dynamics of lipid-bilayer membranes. Our proposal is to divide F into two "monolayer parts", $F = F^{+} + F^{-}$, where

$$F^{\pm} = \oint dA\, \frac{k_{\rm eff}}{2} \cdot \left(\phi^{\pm}\right)^2 \pm \oint dA\, \lambda H \phi^{\pm} + \frac{1}{2}\left\{ \oint dA\, \frac{\kappa_{\rm eff}}{2}(2H)^2 + \sigma_0 \oint dA \right\} \tag{24}$$

is associated with a single monolayer, and then to derive the corresponding restoring force from the variation of the monolayer free energy. This definition is consistent with the bilayer-composite structure of the vesicle membrane.

The second is the issue of how to deal with the variations in the monolayer density fields $\rho^{+}(u^1,u^2,t)$ and $\rho^{-}(u^1,u^2,t)$ in their relations to the shape variations of the monolayer surfaces. Our proposal [2] concerning this issue is that the number of molecules associated with any local area element dA of a monolayer should be conserved under the shape variation of the monolayer. In other words,

$$\delta(dA\, \rho^{\pm}) = 0 \,. \tag{25}$$

The reason for this lies in the basic thermodynamic consideration that the variation in the free energy should be equal to the *mechanical* work done against the restoring forces. Briefly, in considering the hydrodynamics of the membrane surface, we assume that the thermodynamics of a local monolayer element with area dA and $N^{\pm}_{\Delta}$ number of molecules is described by the local free energy

$$F^{\pm}_{\Delta}(T, N^{\pm}_{\Delta}, dA(\boldsymbol{R}), \boldsymbol{R}) = dA\, \left\{ \frac{k_{\rm eff}}{2} \cdot \left(\phi^{\pm}\right)^2 + \frac{\sigma_0}{2} \right\} + dA\, \left\{ \frac{\kappa_{\rm eff}}{4}(2H)^2 \pm \lambda H \phi^{\pm} \right\} \,. \tag{26}$$

Clearly, the change in the local free energy, which can be identified with mechanical work, must be the change under constant T and constant $N^{\pm}_{\Delta}$.

The mathematical derivation of the restoring forces for a vesicle of arbitrary shape is similar to that described by Jenkins [27] and is somewhat lengthy. We will only state the final result here:

$$\boldsymbol{f}^{\pm}_{\rm rs} = \Big\{ -\kappa_{\rm eff}\left[H\left(2H^2 - 2K\right) + \Delta H\right] - \pi^{\pm}(2H) \mp \lambda\left[\frac{1}{2}\Delta\phi^{\pm} + (2H^2 - K)\phi^{\pm} + 2H^2\right] \Big\}\boldsymbol{n} - \boldsymbol{\nabla}_{\rm t}\pi^{\pm} \mp \lambda(1+\phi^{\pm})\boldsymbol{\nabla}_{\rm t} H \,, \tag{27}$$

where $\Delta \equiv (1/\sqrt{a})\partial_\alpha(a^{\alpha\beta}\sqrt{a}\partial_\beta)$ is the Laplace-Beltrami operator, $\boldsymbol{\nabla}_{\rm t} \equiv \boldsymbol{t}_\beta a^{\alpha\beta}\partial_\alpha$ is the gradient operator defined on the surface, and $\pi_{\pm} \equiv -\dfrac{\sigma_0}{2} + k_{\rm eff}\phi^{\pm} + \dfrac{k_{\rm eff}}{2}\left(\phi^{\pm}\right)^2$ may be considered as monolayer surface pressures under the condition of planar geometry.

3.2.2 Hydrodynamic forces due to the bulk fluids

The hydrodynamic forces exerted on the monolayers by their corresponding bulk fluids can be determined by solving the equations of motion for the two bulk fluids separated by the membrane under appropriate boundary conditions.

Equations of motion

Since the bulk solvents for lipid-bilayer vesicles are always aqueous, it is a good approximation to consider the fluids as being incompressible. Let the velocity and pressure

[2] Our proposal appears to be the same as that used in Ref. [22].

fields in the two bulk fluids be represented by $\boldsymbol{v}^{(\mathrm{o})}(\boldsymbol{r},t)$, $\boldsymbol{v}^{(\mathrm{i})}(\boldsymbol{r},t)$, and $p^{(\mathrm{o})}(\boldsymbol{r},t)$, $p^{(\mathrm{i})}(\boldsymbol{r},t)$, respectively, where the superscript "o" refers to the bulk fluid outside the vesicle and in contact with the (+)-monolayer and the superscript "i" refers to the bulk fluid inside the vesicle and in contact with the (−)-monolayer. It is then straightforward to write down the hydrodynamic equations:

$$\nabla\cdot\boldsymbol{v}^{(\mathrm{a})}=0\;, \tag{28}$$

$$\rho_{\mathrm{b}}\left[\frac{\partial\boldsymbol{v}^{(\mathrm{a})}}{\partial t}+(\boldsymbol{v}^{(\mathrm{a})}\cdot\nabla)\boldsymbol{v}^{(\mathrm{a})}\right]=-\nabla p^{(\mathrm{a})}+\eta\nabla^2\boldsymbol{v}^{(\mathrm{a})}\;, \tag{29}$$

where ρ_{b} and η are the mass density and the shear viscosity of the bulk fluids, respectively, and the superscript $\mathrm{a}=\mathrm{i},\mathrm{o}$.

Boundary conditions: kinematic matching

Each monolayer of the vesicle provides a boundary surface for the corresponding bulk fluid. Boundary conditions, which specify $\boldsymbol{V}^{(\mathrm{a})}(u^1,u^2,t)\equiv\boldsymbol{v}^{(\mathrm{a})}(\boldsymbol{r}=\boldsymbol{R}(u^1,u^2,t),t)$, are required for completely determining solutions to the above equations. Under very general circumstances, $\boldsymbol{V}^{(\mathrm{a})}$ may be different from the flow velocity in the corresponding monolayer, $\boldsymbol{U}^{\pm}(u^1,u^2,t)$. In the absence of any practical evidence for the general scenario, we choose to match the bulk kinematics at the boundary surfaces with the monolayer surface kinematics, i.e.,

$$\boldsymbol{V}^{(\mathrm{o})}(u^1,u^2,t)=\boldsymbol{U}^{+}(u^1,u^2,t)\;, \tag{30}$$

$$\boldsymbol{V}^{(\mathrm{i})}(u^1,u^2,t)=\boldsymbol{U}^{-}(u^1,u^2,t)\;. \tag{31}$$

Bulk hydrodynamic forces

Once the complete solutions to the bulk hydrodynamic equations are obtained, the corresponding hydrodynamic stress tensors, $\mathsf{T}^{(\mathrm{a})}$, are readily derived as,

$$\mathsf{T}^{(\mathrm{a})}(\boldsymbol{r},t)=-p^{(\mathrm{a})}(\boldsymbol{r},t)\mathbf{I}+\eta\left[\nabla\boldsymbol{v}^{(\mathrm{a})}(\boldsymbol{r},t)+(\nabla\boldsymbol{v}^{(\mathrm{a})}(\boldsymbol{r},t))^{\mathsf{T}}\right], \tag{32}$$

where $\mathbf{I}$ is the unit tensor, and the superscript "T" indicates the transpose of a tensor. The forces per unit area exerted on the two monolayers by the corresponding bulk fluids can finally be evaluated as follows,

$$\boldsymbol{T}^{+}(u^1,u^2,t)=\left.\mathsf{T}^{(\mathrm{o})}(\boldsymbol{r},t)\right|_{\boldsymbol{r}=\boldsymbol{R}(u^1,u^2,t)}\cdot\boldsymbol{n}(u^1,u^2,t)\;,$$

$$\boldsymbol{T}^{-}(u^1,u^2,t)=-\left.\mathsf{T}^{(\mathrm{i})}(\boldsymbol{r},t)\right|_{\boldsymbol{r}=\boldsymbol{R}(u^1,u^2,t)}\cdot\boldsymbol{n}(u^1,u^2,t)\;,$$

where $\boldsymbol{n}(u^1,u^2,t)$ indicates the local normal vector of the membrane surface that directs towards the exterior of the vesicle.

4 Dynamics of shape fluctuations of quasi-spherical vesicles

Having formulated in the previous sections a systematic and general theory for near-equilibrium dynamics of lipid-bilayer vesicles, we will in this section present the application of the theory to systems of quasi-spherical vesicles. By quasi-spherical vesicles, we refer to those vesicles with very small excess areas such that their equilibrium shapes are spherical. Thus, both equilibrium shape fluctuations and non-equilibrium shape deformations may be considered as small perturbations around the spherical equilibrium shapes. Under such conditions, an analytical rendering of the theory becomes possible, provided that certain approximations are made.

4.1 Quasi-spherical vesicles: specific notations

For describing the surface geometry of a quasi-spherical vesicle in the embedding three-dimensional space, the most convenient coordinate system is the spherical coordinate system (θ,φ,r), with local unit basis vectors $\boldsymbol{e}_\theta$, $\boldsymbol{e}_\varphi$, and $\boldsymbol{e}_r$. The quasi-spherical geometry of the membrane surface of the vesicle can be represented by

$$\boldsymbol{R}(\theta,\varphi,t)=R(\theta,\varphi,t)\boldsymbol{e}_r=R_0[\,1+u(\theta,\varphi,t)\,]\boldsymbol{e}_r\;, \tag{33}$$

where R_0 is the radius of the spherical equilibrium shape, and $u(\theta,\varphi,t)$ describes an arbitrary, small shape perturbation. The two local tangent vectors on the quasi-spherical surface are then given by

$$\begin{aligned}\boldsymbol{t}_\theta&\equiv\frac{\partial\boldsymbol{R}}{\partial\theta}=R\boldsymbol{e}_\theta+R_\theta\boldsymbol{e}_r\\ \boldsymbol{t}_\varphi&\equiv\frac{\partial\boldsymbol{R}}{\partial\varphi}=R\sin\theta\boldsymbol{e}_\varphi+R_\varphi\boldsymbol{e}_r\;,\end{aligned} \tag{34}$$

where $R_\theta\equiv\partial R/\partial\theta=R_0\;\partial u/\partial\theta$ and $R_\varphi\equiv\partial R/\partial\varphi=R_0\;\partial u/\partial\varphi$.

It follows from Eq.(16) that for this geometry, the covariant components of the velocity of each monolayer can be found as

$$U^{\alpha}_{\pm}=W^{\alpha}_{\pm}+a^{\alpha\beta}(\boldsymbol{t}_\beta\cdot\boldsymbol{e}_r)\partial_t R=W^{\alpha}_{\pm}+a^{\alpha\beta}R_\beta\partial_t R\;.$$

Clearly, in the scheme of linearization where quantities are expressed accurate only to first order in the perturbation represented by u,

$$\boldsymbol{U}^{\pm}_{\mathrm{t}}=U^{\alpha}_{\pm}\boldsymbol{t}_\alpha=R_0\;W^{\theta}_{\pm}\boldsymbol{e}_\theta+(R_0\sin\theta)\;W^{\varphi}_{\pm}\boldsymbol{e}_\varphi\;. \tag{35}$$

The components of $\boldsymbol{U}_{\pm}=U^{\pm}_{\theta}\boldsymbol{e}_\theta+U^{\pm}_{\varphi}\boldsymbol{e}_\varphi+U^{\pm}_{r}\boldsymbol{e}_r$ will also be needed later and are expressed here as well to first order in the perturbation

$$\begin{aligned}U^{\pm}_{\theta}(\theta,\varphi,t)&=R_0W^{\theta}_{\pm}(\theta,\varphi,t)\;,\\ U^{\pm}_{\phi}(\theta,\varphi,t)&=R_0\sin\theta W^{\varphi}_{\pm}(\theta,\varphi,t)\;,\\ U^{\pm}_{r}(\theta,\varphi,t)&=R_0\dot{u}(\theta,\varphi,t)\;,\end{aligned} \tag{36}$$

where we have introduced a short-hand notation, $\dot{g}(t)=\partial g(t)/\partial t$, for the time derivative of any function $g(t)$. Another quantity to collect here is $D_\alpha W^{\alpha}_{\pm}$. Within the scheme of linearization,

$$D_\alpha W^{\alpha}_{\pm}=D^{(0)}_{\alpha}W^{\alpha}_{\pm}=\left(\frac{\partial W^{\theta}_{\pm}}{\partial\theta}+\cot\theta W^{\theta}_{\pm}+\frac{\partial W^{\varphi}_{\pm}}{\partial\varphi}\right)\;. \tag{37}$$

Two differential operators will be defined here for later use,

$$\boldsymbol{\nabla}_{\rm L} \equiv \boldsymbol{e}_\theta \frac{\partial}{\partial\theta} + \boldsymbol{e}_\varphi \frac{1}{\sin\theta}\cdot\frac{\partial}{\partial\varphi}\ , \tag{38}$$

and $\hat{L}^2 \equiv -\boldsymbol{\nabla}_{\rm L}\cdot\boldsymbol{\nabla}_{\rm L}$. Clearly, by invoking $\hat{L}^2$ on the spherical harmonics, $\mathcal{Y}_{\ell m}$, we have

$$\hat{L}^2\mathcal{Y}_{\ell m} = \ell(\ell+1)\mathcal{Y}_{\ell m}\ . \tag{39}$$

Finally, we write down the expansions of all the relevant fields, $u(\theta,\varphi,t)$ and $\phi^{\pm}(\theta,\varphi,t)$ in the basis of the spherical harmonics, $\mathcal{Y}_{\ell m}(\theta,\varphi)$,

$$\begin{aligned} u(\theta,\varphi,t) &= {\sum_{\ell,m}}' u_{\ell m}(t)\ \mathcal{Y}_{\ell m} \\ &\equiv \sum_{\ell=2}\sum_{m=-\ell}^{m=\ell} u_{\ell m}(t)\ \mathcal{Y}_{\ell m}\ , \end{aligned} \tag{40}$$

$$\begin{aligned} \phi^{\Delta}(\theta,\varphi,t) &= \phi_0^{\Delta} + {\sum_{\ell,m}}' \psi^{\Delta}_{\ell m}(t)\ \mathcal{Y}_{\ell m} \\ &\equiv \phi_0^{\Delta} + \sum_{\ell=2}\sum_{m=-\ell}^{m=\ell} \psi^{\Delta}_{\ell m}(t)\ \mathcal{Y}_{\ell m}\ , \end{aligned} \tag{41}$$

$$\begin{aligned} \phi^{\Sigma}(\theta,\varphi,t) &= \phi_0^{\Sigma} + {\sum_{\ell,m}}' \psi^{\Sigma}_{\ell m}(t)\ \mathcal{Y}_{\ell m} \\ &\equiv \phi_0^{\Sigma} + \sum_{\ell=2}\sum_{m=-\ell}^{m=\ell} \psi^{\Sigma}_{\ell m}(t)\ \mathcal{Y}_{\ell m}\ . \end{aligned} \tag{42}$$

where two alternative fields

$$\phi^{\Delta}(\theta,\varphi,t) \equiv \frac{\phi^{+}(\theta,\varphi,t) - \phi^{-}(\theta,\varphi,t)}{2}\ , \tag{43}$$

$$\phi^{\Sigma}(\theta,\varphi,t) \equiv \frac{\phi^{+}(\theta,\varphi,t) + \phi^{-}(\theta,\varphi,t)}{2}\ , \tag{44}$$

are used instead of $\phi^{\pm}(\theta,\varphi,t)$ for later convenience. $\phi_0^{\Delta} \equiv (\phi_0^{+} - \phi_0^{-})/2$, and $\phi_0^{\Sigma} \equiv (\phi_0^{+} + \phi_0^{-})/2 = 0$ are constants characterizing the equilibrium state of the vesicle; and $\{u_{\ell m}(t), \psi^{\Delta}_{\ell m}(t), \psi^{\Sigma}_{\ell m}(t)\}$ represent the perturbations.

The reasons for not including $\ell = 0, 1$ modes in the above expansions may not all appear obvious. The $\ell = 0$ mode is excluded in Eq.(40) because we will not be considering this mode. This is related to the fact that the dynamics of this mode in the fluctuation spectrum is not only slaved by the dynamics of the other modes, but is also unresolvable experimentally. The $\ell = 1$ mode in the perturbation expansion corresponds to a simple translation of the vesicle and its amplitude is thus set to zero without loss of generality. The exclusion of the $\ell = 1$ modes in Eq.(41) and Eq.(42) is due to the fact that they are not coupled to the shape changes of the vesicle within the scheme of small perturbations.

4.2 Approximations

In the application that will be presented in the following, the most significant approximation which has been made is that the near-equilibrium dynamics of the vesicles are purely dissipative, or overdamped. In other words, the inertial effects in both the bulk hydrodynamics and the monolayer surface hydrodynamics are neglected. This approximation has apparently been made in all theoretical work on vesicle dynamics, based on the estimates put forward first by Milner and Safran [7]. Underlying the consideration of Milner and Safran was, however, the assumption that the only relevant dynamics of a membrane vesicle was the dynamics of the membrane conformation. Therefore, although we adopt the same approximation in this paper, we feel that additional considerations to those that led to the earlier estimates are needed, given the fact that in addition to the surface geometry field monolayer density fields are also being considered. Thus, we briefly state this issue here.

Let's consider the bulk hydrodynamics first. Making the approximation amounts to neglecting both the inertial term and the non-linear convective term in the Navier-Stokes equation written in Eq.(28). By estimating the respective ratios of the two terms to the viscous-force term, we may have a guideline on whether the approximation is justified or not. The ratio of the inertial term to the viscous-force term can be measured roughly by a dimensionless quantity

$$\bar{\mathcal{R}} \equiv \frac{\rho_{\rm b} L^2}{\eta t_0} \sim \frac{\rho_{\rm b}|\partial\boldsymbol{v}/\partial t|}{\eta|\nabla^2\boldsymbol{v}|}\ , \tag{45}$$

where L and t_0 are, respectively, the typical length and time scales characterizing the spatial and temporal variations of $\boldsymbol{v}$. Another dimensionless quantity measures the ratio of the convective term to the viscous-force term,

$$\mathcal{R} \equiv \frac{\rho_{\rm b} v L}{\eta} \sim \frac{\rho_{\rm b}|(\boldsymbol{v}\cdot\nabla)\boldsymbol{v}|}{\eta|\nabla^2\boldsymbol{v}|}\ .$$

This quantity is the conventionally defined Reynolds number [28].

In the case of vesicle dynamics, motions in the bulk fluids are induced by motions of the vesicle membranes, which may be considered as a linear composition of modes of motion characterized by different wavelengths. For each given mode $L = \alpha\ \mu$m should correspond to the characteristic wavelength of the mode. For a vesicle of 20μm radius, α may range from 1 to 60, covering those modes that can be resolved under optical microscope. For a self-consistency check of the no-inertia approximation, the time scale t_0 should represent the shortest time scale characterizing the overdamped dynamics of a vesicle, rather than simply the time scale associated with the overdamped relaxation of a pure bending mode, as was the case considered by Milner and Safran [7]. For pedagogical reasons, we will leave the quantitative self-consistency check to the discussion, where more understanding of the various relaxation time scales will have become available.

To estimate the order of magnitude of $\mathcal{R}$, we replace v by l/t_0, where l should be a measure of the shape deformations of the vesicles from their equilibrium shapes, and is always much smaller than L in the cases that we are interested in. Consequently, we have $\mathcal{R}/\bar{\mathcal{R}} = l/L \ll 1$. Based

on this analysis, we may always neglect the convective term in our considerations of near-equilibrium dynamics of vesicles, provided that $\mathcal{R}$ is smaller than 1. Equations (28) thus become

$$\nabla \cdot \boldsymbol{v}^{(\mathrm{a})} = 0 \,, \\ \nabla p^{(\mathrm{a})} = \eta \nabla^2 \boldsymbol{v}^{(\mathrm{a})} \,, \tag{46}$$

Similar order-of-magnitude analysis can be made regarding the approximation of neglecting the inertial and convective terms in the two-dimensional counterpart of the bulk Navier-Stokes equation, Eq.(19). The order of magnitude of the surface inertial term is given by $\rho_{\mathrm{m}}|\boldsymbol{U}|/t_0$, where ρ_{m} is the surface mass density of a lipid monolayer, and the order of magnitude of the forces acting on a monolayer may be represented by $|\boldsymbol{T}| \sim \eta v/L \sim \eta|\boldsymbol{U}|/L$. The ratio of these two terms is then given by

$$\mathcal{R}_{\mathrm{m}} = \frac{\rho_{\mathrm{m}} L}{\eta t_0} = \frac{\rho_{\mathrm{m}}/L}{\rho_{\mathrm{b}}} \bar{\mathcal{R}} \,. \tag{47}$$

It is easy to work out that $\mathcal{R}_{\mathrm{m}} \ll \bar{\mathcal{R}}$. Thus, The approximation that the monolayer surface hydrodynamics is overdamped is well justified. Under this approximation, Eq.(19) reduces to

$$\boldsymbol{f}^{\pm} = \boldsymbol{f}^{\pm}_{\mathrm{rs}} + \boldsymbol{T}^{\pm} \mp b\,(\boldsymbol{U}^{+}_{\mathrm{t}} - \boldsymbol{U}^{-}_{\mathrm{t}}) = 0 \,. \tag{48}$$

It is more useful to decompose the above vector equations into their components in the normal and the tangential directions. Moreover, it turns out that, in the normal direction, only the sum of the two monolayer equations is relevant, which reads

$$(\boldsymbol{f}^{+}_{\mathrm{rs}} + \boldsymbol{f}^{-}_{\mathrm{rs}}) \cdot \boldsymbol{n} + (\boldsymbol{T}^{+} + \boldsymbol{T}^{-}) \cdot \boldsymbol{n} = 0 \,. \tag{49}$$

In the tangential directions, the more convenient expressions can be obtained by the difference and the sum of the two monolayer equations, which look like

$$(\boldsymbol{f}^{+}_{\mathrm{rs,t}} - \boldsymbol{f}^{-}_{\mathrm{rs,t}}) + (\boldsymbol{T}^{+}_{\mathrm{t}} - \boldsymbol{T}^{-}_{\mathrm{t}}) - 2b\,(\boldsymbol{U}^{+}_{\mathrm{t}} - \boldsymbol{U}^{-}_{\mathrm{t}}) = 0 \,, \tag{50}$$

$$(\boldsymbol{f}^{+}_{\mathrm{rs,t}} + \boldsymbol{f}^{-}_{\mathrm{rs,t}}) + (\boldsymbol{T}^{+}_{\mathrm{t}} + \boldsymbol{T}^{-}_{\mathrm{t}}) = 0 \,. \tag{51}$$

In principle, the last three equations are applicable to vesicles with arbitrary shapes. In applying these equations to the case of a quasi-spherical vesicle, we will only consider contributions which are first order in the perturbations. The first-order contributions from both $\boldsymbol{f}^{\pm}_{\mathrm{rs}}$ and $\boldsymbol{U}^{\pm}_{\mathrm{t}}$ can be obtained exactly without approximation. The situation concerning $\boldsymbol{T}^{\pm}$ is not as well controlled, since an exact solution would involve solving the bulk hydrodynamic equations for boundaries of arbitrary shapes. A practical approach, which is consistent with the linearization scheme, is to make an approximation,

$$\boldsymbol{T}^{\pm} = \boldsymbol{T}^{\pm}_{0};, \tag{52}$$

where $\boldsymbol{T}^{\pm}_{0}$ is obtained by solving the bulk hydrodynamic equations given in Eq.(46) for spherical boundaries that coincide with the spherical equilibrium shape of the vesicle.

4.3 Mechanical restoring forces

The general expressions for the mechanical restoring forces given in Eq.(27) should be evaluated now for the specific case of the quasi-spherical vesicle described by Eq.(33) to first order in the perturbation fields.

In the scheme of linearization, the mean curvature H and the Gaussian curvature K take on the following forms,

$$H = -\frac{1}{R_0} - \frac{1}{2R_0} {\sum_{\ell,m}}' (\ell+2)(\ell-1) u_{\ell m} \mathcal{Y}\ell m \,, \tag{53}$$

$$K = \frac{1}{R_0^2} + \frac{1}{R_0^2} {\sum_{\ell,m}}' (\ell+2)(\ell-1) u_{\ell m} \mathcal{Y}\ell m \,. \tag{54}$$

The Laplace-Beltrami operator Δ and the surface gradient operator $\boldsymbol{\nabla}_{\mathrm{t}}$ become

$$\Delta = -\frac{\hat{L}^2}{R_0^2} \,, \quad \boldsymbol{\nabla}_{\mathrm{t}} \Phi(\theta,\varphi) = \frac{1}{R_0} \boldsymbol{\nabla}_{\mathrm{L}} \Phi(\theta,\varphi) \,,$$

if $\Phi(\theta,\varphi)$ is any function of first order in the perturbation fields.

By the use of the above simplified expressions, the sum of the two monolayer normal components is evaluated to be

$$\begin{aligned} &(\boldsymbol{f}^{+}_{\mathrm{rs}} + \boldsymbol{f}^{-}_{\mathrm{rs}}) \cdot \boldsymbol{n} \\ &= -\frac{2\bar{\tau}}{R_0} - {\sum_{\ell,m}}' \Big\{ \frac{\kappa_{\mathrm{eff}}}{R_0^3} E_\ell u_{\ell m} - \frac{4k_{\mathrm{eff}}}{R_0} \psi^{\Sigma}_{\ell m} \\ &- \left[4\frac{k_{\mathrm{eff}}}{R_0} \phi_0^{\Delta} + \frac{\lambda}{R_0^2} (\ell+2)(\ell-1) \right] \psi^{\Delta}_{\ell m} \Big\} \mathcal{Y}_{\ell m} \,, \end{aligned} \tag{55}$$

where

$$\bar{\tau} \equiv \sigma_0 + \frac{\lambda \phi_0^{\Delta}}{R_0} - k_{\mathrm{eff}} \left(\phi_0^{\Delta}\right)^2 \,, \tag{56}$$

and

$$E_\ell \equiv (\ell+2)(\ell-1) \left[\ell(\ell+1) + \tau_0 \, \frac{R_0^2}{\kappa_{\mathrm{eff}}} \right] \,, \tag{57}$$

with

$$\tau_0 \equiv \bar{\tau} + \frac{\lambda \phi_0^{\Delta}}{R_0} \,. \tag{58}$$

The two tangential forces, $\boldsymbol{f}^{+}_{\mathrm{rs,t}}$ and $\boldsymbol{f}^{-}_{\mathrm{rs,t}}$, are, to first order in the perturbations, given by

$$\boldsymbol{f}^{\pm}_{\mathrm{rs,t}} = -k_{\mathrm{eff}} (1+\phi_0^{\pm}) \boldsymbol{\nabla}_{\mathrm{L}} \phi^{\pm} \mp \lambda (1+\phi_0^{\pm}) \boldsymbol{\nabla}_{\mathrm{L}} H \,.$$

The really relevant quantities are not the tangential forces themselves, but the following ones,

$$\begin{aligned} \boldsymbol{\nabla}_{\mathrm{L}} \cdot (\boldsymbol{f}^{+}_{\mathrm{rs,t}} - \boldsymbol{f}^{-}_{\mathrm{rs,t}}) = {\sum_{\ell,m}}' \ell(\ell+1) \Big[2\frac{k_{\mathrm{eff}}}{R_0^2} \, \psi^{\Delta}_{\ell m} \\ - \frac{\lambda}{R_0^3} (\ell+2)(\ell-1) u_{\ell m} + \frac{2k_{\mathrm{eff}} \phi_0^{\Delta}}{R_0^2} \psi^{\Sigma}_{\ell m} \Big] \mathcal{Y}_{\ell m} \,, \end{aligned} \tag{59}$$

and

$$\boldsymbol{\nabla}_{\rm L}\cdot(\boldsymbol{f}^{+}_{\rm rs,t}+\boldsymbol{f}^{-}_{\rm rs,t})=\sum_{\ell,m}{}'\ell(\ell+1)\left[2\frac{k_{\rm eff}}{R_0^2}\psi^{\Sigma}_{\ell m}-\frac{\lambda\phi_0^{\Delta}}{R_0^3}(\ell+2)(\ell-1)u_{\ell m}+\frac{2k_{\rm eff}\phi_0^{\Delta}}{R_0^2}\psi^{\Delta}_{\ell m}\right]\mathcal{Y}_{\ell m}\ . \tag{60}$$

4.4 Forces due to the bulk hydrodynamics

The forces, $\boldsymbol{T}_0^{\pm}$, defined in Eq.(52) can be obtained based on an adaptation to our problem of the classical Lamb solution [29]. This approach has already been used in the previous work on vesicle dynamics by Schneider *et al.* [10], Yeung and Evans [16], and Seifert [30]. We will, therefore, only summarize the final results here.

4.4.1 The Lamb solution

In the Lamb solution, an alternative form of the boundary conditions,
$\boldsymbol{v}^{(\rm a)}(r,\theta,\varphi,t)|_{r=R_0}=\boldsymbol{V}^{(\rm a)}(\theta,\varphi,t)$, is adopted, where the following three scalar quantities are used instead of the three components of $\boldsymbol{V}^{(\rm a)}(\theta,\varphi,t)$:

$$\begin{aligned}X^{(\rm a)}(\theta,\varphi,t)&\equiv\boldsymbol{V}^{(\rm a)}(\theta,\varphi,t)\cdot\boldsymbol{e}_r\ ,\\ Y^{(\rm a)}(\theta,\varphi,t)&\equiv-R_0\boldsymbol{\nabla}\cdot\boldsymbol{V}^{(\rm a)}(\theta,\varphi,t)\ ,\\ Z^{(\rm a)}(\theta,\varphi,t)&\equiv R_0\boldsymbol{e}_r\cdot(\boldsymbol{\nabla}\times\boldsymbol{V}^{(\rm a)}(\theta,\varphi,t))\ .\end{aligned} \tag{61}$$

The above three quantities can be expanded in the basis of the spherical harmonics,

$$X^{(\rm a)}(\theta,\varphi,t)=\sum_{\ell,m}{}'\ X^{(\rm a)}_{\ell m}(t)\ \mathcal{Y}_{\ell m}\ , \tag{62}$$

$$Y^{(\rm a)}(\theta,\varphi,t)=\sum_{\ell,m}{}'\ Y^{(\rm a)}_{\ell m}(t)\ \mathcal{Y}_{\ell m}\ , \tag{63}$$

$$Z^{(\rm a)}(\theta,\varphi,t)=\sum_{\ell,m}{}'\ Z^{(\rm a)}_{\ell m}(t)\ \mathcal{Y}_{\ell m}\ . \tag{64}$$

The normal and the tangential components of $\boldsymbol{T}_0^{\pm}$ can now be expressed in terms of $X^{(\rm a)}_{\ell m}(t)$, $Y^{(\rm a)}_{\ell m}(t)$, and $Z^{(\rm a)}_{\ell m}(t)$. The normal components read as

$$\begin{aligned}T^{+}_{0,\rm n}&=-p_0^{(\rm o)}+\frac{\eta}{R_0}\sum_{\ell=2}\sum_{m=-\ell}^{\ell}\frac{-(2\ell^2+3\ell-2)}{\ell+1}\ X^{(\rm o)}_{\ell m}\ \mathcal{Y}_{\ell m}\\ &\quad+\frac{\eta}{R_0}\sum_{\ell=2}\sum_{m=-\ell}^{\ell}\frac{3}{\ell+1}Y^{(\rm o)}_{\ell m}\ \mathcal{Y}_{\ell m}\ ,\\ T^{-}_{0,\rm n}&=p_0^{(\rm i)}-\frac{\eta}{R_0}\sum_{\ell=2}\sum_{m=-\ell}^{\ell}\frac{2\ell^2+\ell-3}{\ell}\ X^{(\rm i)}_{\ell m}\ \mathcal{Y}_{\ell m}\\ &\quad-\frac{\eta}{R_0}\sum_{\ell=2}\sum_{m=-\ell}^{\ell}\frac{3}{\ell}\ Y^{(\rm i)}_{\ell m}\ \mathcal{Y}_{\ell m}\ ,\end{aligned} \tag{65}$$

where $p_0^{(\rm o)}$ and $p_0^{(\rm i)}$ are the hydrostatic pressures in the bulk fluids outside and inside the vesicle, respectively.

When the tangential components, $\boldsymbol{T}^{\pm}_{0,\rm t}$ are concerned, it is more convenient to use $\boldsymbol{\nabla}_{\rm L}\cdot\boldsymbol{T}^{\pm}_{0,\rm t}$, which look like

$$\begin{aligned}\boldsymbol{\nabla}_{\rm L}\cdot\boldsymbol{T}^{+}_{0,\rm t}&=\\ \frac{\eta}{R_0}\sum_{\ell=2}\sum_{m=-\ell}^{\ell}&\left[(\ell+2)X^{(\rm o)}_{\ell m}+(2\ell+1)Y^{(\rm o)}_{\ell m}\right]\mathcal{Y}_{\ell m}\ ,\\ \boldsymbol{\nabla}_{\rm L}\cdot\boldsymbol{T}^{-}_{0,\rm t}&=\\ \frac{\eta}{R_0}\sum_{\ell=2}\sum_{m=-\ell}^{\ell}&\left[(\ell-1)X^{(\rm i)}_{\ell m}+(2\ell+1)Y^{(\rm i)}_{\ell m}\right]\mathcal{Y}_{\ell m}\ .\end{aligned} \tag{66}$$

4.4.2 Surface continuity equations and kinematic matching

The "amplitudes" $X^{(\rm o)}_{\ell m}$, $X^{(\rm i)}_{\ell m}$, $Y^{(\rm o)}_{\ell m}$ and $Y^{(\rm i)}_{\ell m}$ can be directly related to the amplitudes of the three perturbation fields, $u_{\ell m}(t)$ and $\psi^{\pm}_{\ell m}(t)$ as defined in Eqs.(40)-(42). The connections are provided by the two surface continuity equations given in Eq.(18) and by the kinematic-matching conditions given in Eq.(30). Expressed to first order in the perturbations, Eq.(18) read as

$$\begin{aligned}D_\alpha W^{\alpha}_{\pm}=D^{(0)}_{\alpha}W^{\alpha}_{\pm}&=-\frac{\rho_0}{\rho_0^{\pm}}\dot{\phi}^{\pm}(\theta,\varphi,t)-2\dot{u}(\theta,\varphi,t)\\ &=-\frac{1}{1\pm\phi_0^{\Delta}}\ \dot{\phi}^{\pm}(\theta,\varphi,t)-2\dot{u}(\theta,\varphi,t)\ .\end{aligned} \tag{67}$$

Substituting the kinematic-matching conditions Eq.(30) into Eq.(62) and Eq.(63), using the expressions for $\boldsymbol{U}^{\pm}$ given in Eq.(36), we arrive at

$$X^{(\rm o)}(\theta,\varphi,t)=X^{(\rm i)}(\theta,\varphi,t)=R_0\ \dot{u}(\theta,\varphi,t)\ , \tag{68}$$

$$\begin{aligned}Y^{(\rm o)}(\theta,\varphi,t)&=-2R_0\ \dot{u}(\theta,\varphi,t)\\ &\quad-R_0\left[\frac{1}{\sin\theta}\frac{\partial}{\partial\theta}\left(W^{\theta}_{+}\cdot\sin\theta\right)+\frac{\partial W^{\varphi}_{+}}{\partial\varphi}\right]\ ,\end{aligned} \tag{69}$$

$$\begin{aligned}Y^{(\rm i)}(\theta,\varphi,t)&=-2R_0\ \dot{u}(\theta,\varphi,t)\\ &\quad-R_0\left[\frac{1}{\sin\theta}\frac{\partial}{\partial\theta}\left(W^{\theta}_{-}\cdot\sin\theta\right)+\frac{\partial W^{\varphi}_{-}}{\partial\varphi}\right]\ .\end{aligned} \tag{70}$$

Applying Eq.(67) to the last two equations, we finally have

$$\begin{aligned}X^{(\rm o)}_{\ell m}(t)&=X^{(\rm i)}_{\ell m}(t)=R_0\ \dot{u}_{\ell m}(t)\ ,\\ Y^{(\rm o)}_{\ell m}(t)&=\frac{R_0}{1+\phi_0^{\Delta}}\ \dot{\psi}^{+}_{\ell m}(t)\ ,\\ Y^{(\rm i)}_{\ell m}(t)&=\frac{R_0}{1-\phi_0^{\Delta}}\ \dot{\psi}^{-}_{\ell m}(t)\ .\end{aligned} \tag{71}$$

By substituting Eq.(71) into Eq.(65) and Eq.(67), we arrive at the following relevant expressions:

$$T^+_{0,\rm n}+T^-_{0,\rm n}=-(p^{(\rm o)}_0-p^{(\rm i)}_0) +\sum_{\ell,m}{}'\frac{\eta}{\ell(\ell+1)}\Big\{-(4\ell^3+6\ell^2-4\ell-3)\dot u_{\ell m} -\frac{3[1+(2\ell+1)\phi^{\Delta}_0]}{1-(\phi^{\Delta}_0)^2}\dot\psi^{\Delta}_{\ell m}+\frac{3(2\ell+1+\phi^{\Delta}_0)}{1-(\phi^{\Delta}_0)^2}\dot\psi^{\Sigma}_{\ell m}\Big\}\mathcal{Y}_{\ell m}\,, \tag{72}$$

$$\boldsymbol{\nabla}_{\rm L}\cdot(\boldsymbol{T}^+_{0,\rm t}-\boldsymbol{T}^-_{0,\rm t})=\frac{\eta}{R_0}\sum_{\ell,m}{}'\Big[3\dot u_{\ell m}+\frac{2(2\ell+1)}{1-(\phi^{\Delta}_0)^2}\dot\psi^{\Delta}_{\ell m} -\frac{2(2\ell+1)\phi^{\Delta}_0}{1-(\phi^{\Delta}_0)^2}\dot\psi^{\Sigma}_{\ell m}\Big]\mathcal{Y}_{\ell m}\,, \tag{73}$$

$$\boldsymbol{\nabla}_{\rm L}\cdot(\boldsymbol{T}^+_{0,\rm t}+\boldsymbol{T}^-_{0,\rm t})=\frac{\eta}{R_0}\sum_{\ell,m}{}'\Big[(2\ell+1)\dot u_{\ell m} -\frac{2(2\ell+1)\phi^{\Delta}_0}{1-(\phi^{\Delta}_0)^2}\dot\psi^{\Delta}_{\ell m}+\frac{2(2\ell+1)}{1-(\phi^{\Delta}_0)^2}\dot\psi^{\Sigma}_{\ell m}\Big]\mathcal{Y}_{\ell m}\,. \tag{74}$$

4.5 The intermonolayer frictional forces

The evaluation of the intermonolayer frictional forces appearing in Eq.(50) is straightforward. By applying $\boldsymbol{\nabla}_{\rm L}$ on $\boldsymbol{U}^{\pm}_{\rm t}$ given in Eq.(35), we obtain, to first order in the perturbations,

$$\boldsymbol{\nabla}_{\rm L}\cdot\boldsymbol{U}^{\pm}_{\rm t}=R_0\left(\frac{\partial W^{\theta}_{\pm}}{\partial\theta}+\cot\theta W^{\theta}_{\pm}+\frac{\partial W^{\varphi}_{\pm}}{\partial\varphi}\right) =R_0\,(D_\alpha W^{\alpha}_{\pm})=-R_0\left[\frac{\dot\phi^{\pm}}{1\pm\phi^{\Delta}_0}+2\dot u\right], \tag{75}$$

where Eq.(37) and Eq.(67) have been used. It follows immediately that

$$\boldsymbol{\nabla}_{\rm L}\cdot\big[b(\boldsymbol{U}^+_{\rm t}-\boldsymbol{U}^-_{\rm t})\big]=-bR_0(\frac{\dot\phi^+}{1+\phi^{\Delta}_0}-\frac{\dot\phi^-}{1-\phi^{\Delta}_0}) \tag{76}$$

$$=-2bR_0\sum_{\ell,m}{}'\left(\frac{1}{1-(\phi^{\Delta}_0)^2}\dot\psi^{\Delta}_{\ell m}-\frac{\phi^{\Delta}_0}{1-(\phi^{\Delta}_0)^2}\dot\psi^{\Sigma}_{\ell m}\right)\mathcal{Y}_{\ell m}\,.$$

4.6 Equations of motion

A set of 3 linear equations of motion can now be obtained for the three dynamic variables characterizing a particular mode of perturbation, $u_{\ell m}(t)$, $\psi^{\Delta}_{\ell m}(t)$ and $\psi^{\Sigma}_{\ell m}(t)$. Substitution of both Eq.(55) and Eq.(72) into Eq.(49) yields [3]

$$\frac{\eta}{\ell(\ell+1)}\Big[-(4\ell^3+6\ell^2-4\ell-3)\dot u_{\ell m} -\frac{3[1+(2\ell+1)\phi^{\Delta}_0]}{1-(\phi^{\Delta}_0)^2}\dot\psi^{\Delta}_{\ell m}+\frac{3(2\ell+1+\phi^{\Delta}_0)}{1-(\phi^{\Delta}_0)^2}\dot\psi^{\Sigma}_{\ell m}\Big] =\frac{\kappa_{\rm eff}E_\ell}{R_0^3}u_{\ell m}-\left[4\frac{k_{\rm eff}}{R_0}\phi^{\Delta}_0+\frac{\lambda}{R_0^2}(\ell+2)(\ell-1)\right]\psi^{\Delta}_{\ell m} -\frac{4k_{\rm eff}}{R_0}\psi^{\Sigma}_{\ell m}\,. \tag{77}$$

Similarly, combining Eq.(59), Eq.(73) and Eq.(76) based on Eq.(50) leads to

$$\frac{\eta}{\ell(\ell+1)}\Big\{3\dot u_{\ell m}+\Big[2(2\ell+1)+\frac{4bR_0}{\eta}\Big] \cdot\left(\frac{1}{1-(\phi^{\Delta}_0)^2}\dot\psi^{\Delta}_{\ell m}-\frac{\phi^{\Delta}_0}{1-(\phi^{\Delta}_0)^2}\dot\psi^{\Sigma}_{\ell m}\right)\Big\} =\frac{\lambda}{R_0^2}(\ell+2)(\ell-1)u_{\ell m}-2\frac{k_{\rm eff}}{R_0}\psi^{\Delta}_{\ell m}-\frac{2k_{\rm eff}\phi^{\Delta}_0}{R_0}\psi^{\Sigma}_{\ell m}\,, \tag{78}$$

and combining Eq.(60) and Eq.(74) according to Eq.(51) gives

$$\frac{\eta}{\ell(\ell+1)}\Big[(2\ell+1)\dot u_{\ell m}-\frac{2(2\ell+1)\phi^{\Delta}_0}{1-(\phi^{\Delta}_0)^2}\dot\psi^{\Delta}_{\ell m} +\frac{2(2\ell+1)}{1-(\phi^{\Delta}_0)^2}\dot\psi^{\Sigma}_{\ell m}\Big] =\frac{\lambda\phi^{\Delta}_0}{R_0^2}(\ell+2)(\ell-1)u_{\ell m}-\frac{2k_{\rm eff}\phi^{\Delta}_0}{R_0}\psi^{\Delta}_{\ell m}-2\frac{k_{\rm eff}}{R_0}\psi^{\Sigma}_{\ell m}\,. \tag{79}$$

In principle three independent modes of dynamics can now be determined by solving the three equations of motion given above.

A closer analysis of the equations shows, however, that only two modes of the three are relevant on the time scales that are experimentally accessible, due to the fact that there is an inherent separation of time scales involved in the problem. Three basic time scales may be defined based on Eq.(77), Eq.(78), and Eq.(79),

$$t_{\rm c}=\frac{\eta R_0^3}{\kappa_{\rm eff}}\,\frac{\ell^3}{\ell(\ell+1)E_\ell}\,,\quad t_{\Delta}=\frac{2bR_0^2}{k_{\rm eff}}\,\frac{1}{\ell(\ell+1)}\,, \quad t_{\Sigma}=\frac{\eta R_0}{k_{\rm eff}}\,\frac{(2\ell+1)}{\ell(\ell+1)}\,. \tag{80}$$

An order-of-magnitude estimate based on

$$\kappa_{\rm eff}=10^{-12}\,{\rm erg}\,,\quad k_{\rm eff}=30\,\frac{\rm erg}{\rm cm^2}\,, \tag{81}$$

$$b=5\times10^7\frac{\rm erg\cdot s}{\rm cm^4}\,,\quad R_0=10\,\mu{\rm m}\,,\quad \frac{\tau_0R_0^2}{\kappa_{\rm eff}}=10\,,$$

[3] The equation at the zeroth order is given by $p^{(\rm i)}_0-p^{(\rm o)}_0=2\bar\tau/R_0$.

yields for $\ell = 2$,

$$t_{\rm c} \sim 0.2\ {\rm s}\ , \quad t_{\Delta} \sim 0.5\ {\rm s}\ , \quad t_{\Sigma} \sim 2 \times 10^{-7}\ {\rm s}\ .$$

Clearly, the relaxation of $\psi^{\Sigma}_{\ell m}$, which is characterized by t_{Σ}, is much faster than the relaxations of $u_{\ell m}$ and $\psi^{\Delta}_{\ell m}$. Thus, we can assume

$$\dot{\psi}^{\Sigma}_{\ell m} \simeq 0\ , \tag{82}$$

over the time scales that characterize the relaxations of the slower modes. Using then Eq.(79) to eliminate $\psi^{\Sigma}_{\ell m}$ from the other two equations, we arrive finally at two relevant equations of motion, written in the following in a matrix form

$$\begin{pmatrix} \dot{u}_{\ell m} \\ \dot{\psi}^{\Delta}_{\ell m} \end{pmatrix} = \mathsf{A}^{-1}_{2\times 2}\mathsf{B}_{2\times 2} \begin{pmatrix} u_{\ell m} \\ \psi^{\Delta}_{\ell m} \end{pmatrix} \equiv -\mathsf{C}_{2\times 2} \begin{pmatrix} u_{\ell m} \\ \psi^{\Delta}_{\ell m} \end{pmatrix}\ . \tag{83}$$

The two coefficient matrices are defined as

$$\mathsf{A}_{2\times 2} = \begin{pmatrix} \Gamma_{\ell} & \dfrac{3-(2\ell+1)\phi^{\Delta}_0}{1-(\phi^{\Delta}_0)^2} \\ -3+\beta_{\ell}\phi^{\Delta}_0 & -\dfrac{4b_0+2\beta_{\ell}(1+(\phi^{\Delta}_0)^2)}{1-(\phi^{\Delta}_0)^2} \end{pmatrix}\ , \tag{84}$$

and

$$\mathsf{B}_{2\times 2} = \frac{\ell(\ell+1)}{t_0} \begin{pmatrix} -E_{\ell}+2\phi^{\Delta}_0\lambda_{\ell} & \lambda_{\ell} \\ -\lambda_{\ell}\left[1-(\phi^{\Delta}_0)^2\right] & 2k_0\left[1-(\phi^{\Delta}_0)^2\right] \end{pmatrix}\ , \tag{85}$$

where $t_0 \equiv \eta R_0^3/\kappa_{\rm eff}$ defines a time scale, and

$$b_0 \equiv \frac{bR_0}{\eta}\ , \quad \lambda_0 \equiv \frac{\lambda R_0}{\kappa_{\rm eff}}\ , \quad k_0 \equiv \frac{k_{\rm eff}R_0^2}{\kappa_{\rm eff}}\ ,$$

are dimensionless parameters, and where a few short-hand notations have also been defined

$$\begin{aligned} &\Gamma_{\ell} \equiv (2\ell+1)(2\ell^2+2\ell-1)\ , \quad \beta_{\ell} \equiv 2\ell+1\ , \\ &\lambda_{\ell} \equiv \lambda_0(\ell-1)(\ell+2)\ . \end{aligned} \tag{86}$$

Further approximations can be made in the analysis of Eq.(83). The dimensionless parameters b_0 and k_0 acquire rather large values for those values of the physical parameters quoted in Eq.(81), specifically, $b_0 \approx 5\times 10^6$, and $k_0 \approx 3\times 10^7$, whereas parameter ϕ^{Δ}_0 is expected to be much smaller than one. Thus, both $\mathsf{A}_{2\times 2}$ and $\mathsf{B}_{2\times 2}$ can be simplified as

$$\begin{aligned} \mathsf{A}_{2\times 2} &\cong \begin{pmatrix} \Gamma_{\ell} & 0 \\ 0 & -4b_0 \end{pmatrix}\ , \\ \mathsf{B}_{2\times 2} &\cong \frac{\ell(\ell+1)}{t_0} \begin{pmatrix} -E_{\ell}+2\phi^{\Delta}_0\lambda_{\ell} & \lambda_{\ell} \\ -\lambda_{\ell} & 2k_0 \end{pmatrix}\ . \end{aligned} \tag{87}$$

This yields a rather simple form for matrix $\mathsf{C}_{2\times 2}$,

$$\begin{aligned} \mathsf{C}_{2\times 2} &\cong \frac{\ell(\ell+1)}{4b_0\Gamma_{\ell}t_0} \begin{pmatrix} 4b_0\left(E_{\ell}-2\phi^{\Delta}_0\lambda_{\ell}\right) & -4b_0\lambda_{\ell} \\ -\lambda_{\ell}\Gamma_{\ell} & 2k_0\Gamma_{\ell} \end{pmatrix} \\ &\equiv \begin{pmatrix} \mathsf{C}_{11} & \mathsf{C}_{12} \\ \mathsf{C}_{21} & \mathsf{C}_{22} \end{pmatrix}\ . \end{aligned} \tag{88}$$

A comment is worth making here, which should help clarify the connections between our theory and the previous theories on the vesicle dynamics [7,10,16]. It concerns the two approximations made by use of Eq.(82) and Eq.(87). The first approximation is actually equivalent to imposing the so-called "local area incompressibility constraint" that has been used in some of the previous works [7,10,16]. The physical reason underlying the approximation, expressed in Eq.(82), thus provides a rationale for the use of the constraint. However, it is incorrect, in our opinion, to interpret in general, as the authors of Ref. [16] did, this constraint as representing incompressibility of the monolayers as fluids, to be understood in a way similar to the concept of incompressibility of bulk fluids, since the constraint eliminates only one of the two mechanisms by which the monolayer density fields can change – the mechanism through changes of local surface geometry of the monolayers. The second approximation implies that, as far as the induced hydrodynamic motions in the bulk fluids are concerned, the surface flow effects that are associated with the overall compressibility of the monolayers are negligible. This approximation has the same effect as the approximation used in Ref. [16] (the second equation in Eq. (A.6) therein).

4.7 Dissipative dynamics of shape fluctuations

Finally, two dispersion relations, which characterize the two independent dissipative modes of the vesicle dynamics, can be obtained as the two eigenvalues of $\mathsf{C}_{2\times 2}$,

$$\begin{aligned} \Omega_{\pm}(\ell) = &\frac{1}{2}\left[\Omega_{\rm c}(\ell)+\Omega_{\Delta}(\ell)\right] \\ &\cdot\left[1 \pm \sqrt{1-4\frac{\Omega_{\Delta}(\ell)\cdot\Omega_{\rm a}(\ell)}{\left[\Omega_{\rm c}(\ell)+\Omega_{\Delta}(\ell)\right]^2}}\ \right]\ , \end{aligned} \tag{89}$$

where

$$\begin{aligned} &\Omega_{\Delta}(\ell) \equiv \mathsf{C}_{22} = \frac{\ell(\ell+1)k_{\rm eff}}{2bR_0^2}\ , \\ &\Omega_{\rm c}(\ell) \equiv \mathsf{C}_{11} = \frac{\ell(\ell+1)(\ell-1)(\ell+2)}{\eta R_0^3\Gamma_{\ell}}\left[\ell(\ell+1)\kappa_{\rm eff}+E_{\sigma}\right]\ , \\ &\Omega_{\rm a}(\ell) \equiv \frac{\ell(\ell+1)(\ell-1)(\ell+2)}{\eta R_0^3\Gamma_{\ell}}\left[\ell(\ell+1)\kappa_{\rm a}+E_{\sigma}+\frac{\lambda^2}{k_{\rm eff}}\right]\ . \end{aligned} \tag{90}$$

In the above expressions, the definition

$$E_{\sigma} \equiv R_0^2[\sigma_0 - k_{\rm eff}(\phi^{\Delta}_0)^2] \tag{91}$$

has been used, and

$$\kappa_{\rm a} \equiv \kappa_{\rm eff} - \frac{\lambda^2}{2k_{\rm eff}} \tag{92}$$

defines a new bending rigidity, which will be called "apparent" bending rigidity.

At this stage, the quantity of our main concern, namely, the time-dependent correlation function of shape fluctuations of a quasi-spherical vesicle, $\langle u^*_{\ell m}(t)u_{\ell m}(0)\rangle$, may be written generally as

$$\frac{\langle u^*_{\ell m}(t)u_{\ell m}(0)\rangle}{\langle |u_{\ell m}|^2\rangle} = \beta_- e^{-\Omega_- t} + \beta_+ e^{-\Omega_+ t} \ . \qquad (93)$$

Clearly, $\beta_- + \beta_+ = 1$. To obtain analytical expressions for the amplitudes, $\beta_\mp$, we employ Onsager's regression hypothesis that the equations of motion governing the macroscopic near-equilibrium dynamics can be applied to the dynamics of spontaneous fluctuations [19]. Following the formalism given in Ref. [31] we thus have

$$\langle u^*_{\ell m}(t)u_{\ell m}(0)\rangle = \langle |u_{\ell m}|^2\rangle \ (e^{-\mathsf{C}t})_{11} + \langle u^*_{\ell m}\psi^{\Delta}_{\ell m}\rangle \ (e^{-\mathsf{C}t})_{21} \ , \qquad (94)$$

which leads to the following specific expressions for $\beta_\mp$:

$$\begin{aligned}
\beta_- &= \frac{1}{\Omega_+ - \Omega_-}\left[\Omega_\Delta - \Omega_- - \mathsf{C}_{21}\frac{\langle u^*_{\ell m}\psi^{\Delta}_{\ell m}\rangle}{\langle |u_{\ell m}|^2\rangle}\right] \\
&= \frac{1}{\Omega_+ - \Omega_-}\left[\Omega_\Delta - \Omega_- + \Omega_\Delta \ \left(\frac{\lambda(\ell-1)(\ell+2)}{2k_{\rm eff}R_0}\right)^2\right] \ , \\
\beta_+ &= \frac{1}{\Omega_+ - \Omega_-}\left[\Omega_+ - \Omega_\Delta + \mathsf{C}_{21}\frac{\langle u^*_{\ell m}\psi^{\Delta}_{\ell m}\rangle}{\langle |u_{\ell m}|^2\rangle}\right] \qquad (95) \\
&= \frac{1}{\Omega_+ - \Omega_-}\left[\Omega_+ - \Omega_\Delta - \Omega_\Delta \ \left(\frac{\lambda(\ell-1)(\ell+2)}{2k_{\rm eff}R_0}\right)^2\right] \ .
\end{aligned}$$

$\langle |u_{\ell m}|^2\rangle$ and $\langle u^*_{\ell m}\psi^{\Delta}_{\ell m}\rangle$ represent some of the static correlation functions, the calculations of which are briefly sketched in **Appendix A**.

5 Discussion

The dispersion relations, Eq.(89), predicted by our theory appear *formulistically* identical to those worked out by Yeung and Evans [16] and by Bivas *et al.* [17]. But, our definitions of two of the three quantities involved in the dispersion relations, namely, $\Omega_{\rm c}(\ell)$ and $\Omega_{\rm a}(\ell)$, differ in detail from those previous results. More importantly, we feel that interpretations of those physical parameters contained in the dispersion relations, $\kappa_{\rm eff}$, $k_{\rm eff}$, λ and E_σ, need to be reconsidered.

We have already remarked on the issue of interpretation in Section 2.2, when introducing the effective free energy describing a vesicle with a coarse-grained configuration characterized by $\boldsymbol{R}(u^1,u^2,t)$, and $\rho^{\pm}(u^1,u^2,t)$. As we have not yet performed for systems of quasi-spherical vesicles the coarse-graining procedure similar to those described in Refs. [22,23], we are only able to give a semi-quantitative discussion of the effective mesoscopic parameters.

If we consider systems of quasi-spherical vesicles where fluctuations about equilibrium shapes are small, where a Gaussian theory would suffice in describing the small-scale fluctuations, we may argue that the renormalization of bending rigidity due to nonlinearities [32] can be neglected and that $\kappa_{\rm eff} \simeq \kappa_{\rm m} - \lambda^2_{\rm m}/2k_{\rm m}$, where $\kappa_{\rm m}$, $\lambda_{\rm m}$, and $k_{\rm m}$ represent the phenomenological parameters corresponding the microscopic cut-off length scale. Note that the part subtracted from $\kappa_{\rm m}$ arises from the coupling between membrane curvature field and the density-difference field [21]. But, making a quantitative statement about $\kappa_{\rm eff}$ is not trivial, at least, not straightforward, even from the point of view of experiments. In the so-called flicker-noise analysis experiments, a bending rigidity κ and a "surface-tension" constant $\Sigma_{\rm e}$ are inferred from fitting the experimental data on $\langle |\hat{u}_{\ell m}|^2\rangle$ onto a functional expression,

$$\langle |\hat{u}_{\ell m}|^2\rangle = \frac{k_{\rm B}T}{(\ell-1)(\ell+2)\kappa[\ell(\ell+1)+\Sigma_{\rm e}]} \ . \qquad (96)$$

Based on our theory and calculations presented in Appendix A, which yields

$$\langle |\hat{u}_{\ell m}|^2\rangle = \frac{k_{\rm B}T}{(\ell-1)(\ell+2)\kappa_{\rm a}[\ell(\ell+1)+\Sigma]} \ , \qquad (97)$$

where

$$\Sigma \equiv \frac{1}{\kappa_{\rm a}}\left[\sigma_0 R_0^2 - k_{\rm eff}R_0^2(\phi_0^{\Delta})^2 + \frac{\lambda^2}{k_{\rm eff}}\right] \ , \qquad (98)$$

the experimentally obtained bending rigidity κ should be identified not with $\kappa_{\rm eff}$, but with $\kappa_{\rm a}$, the apparent or renormalized bending rigidity.

$k_{\rm eff}$ is expected to be lower than its microscopic counterpart due to the renormalization effect when the vesicles are either in or close to the *floppy* states, as we have already mentioned in Section 2.2. It is our opinion that the values of area compressibility moduli for various single-component membrane systems reported so far in the literature [25,33] are actually the values of the microscopic area compressibility moduli, as these values have been obtained when the membranes under observation are in *stretched-tense* states [23]. In the absence of any available experimental data on $k_{\rm eff}$, we make an estimate based on the semi-quantitative derivation of the parameter given in Ref. [23] by using a short-distance cut-off of optical lengths, $\Lambda^{-1} = 100$ nm and obtain $k_{\rm eff} \simeq 30$ erg/cm^2. This value is lower by 2-3 fold than the values of the microscopic area compressibility moduli typically quoted in the literature .

The parameter, λ, is a rather elusive one, due to the fact that understanding of the physical origin of $\lambda_{\rm m}$ is limited. We will follow the discussion on it put forward by Seifert and Langer [15] and put an estimate on $\lambda_{\rm m}$ as $\lambda_{\rm m} = 2k_{\rm m}d$, where $d \simeq 1$nm, representing roughly half of the monolayer thickness. Taking $d \simeq 1$ nm and $k_{\rm m} = 100$ erg/cm^2, we have $\lambda_{\rm m} \simeq 2\times 10^{-5}$ erg/cm. It is not difficult to see, if one follows the kind of coarse-graining procedures described in [22], that $\lambda \simeq \lambda_{\rm m}$.

The parameter, E_σ, should according to our calculation be related to the experimentally inferred parameter $\Sigma_{\rm e}$:

$$E_\sigma = \kappa_{\rm a}\Sigma_{\rm e} - \frac{\lambda^2}{k_{\rm eff}} \ , \qquad (99)$$

as, based on Eq.(96) and Eq.(97), Σ should be identified with $\Sigma_{\rm e}$.

Our analytical expressions for $\beta_{\mp}$ differ also qualitatively both from those given in Ref. [16] and from those given in Ref. [17]. Explicitly, the qualitative corrections to the expressions given in Ref. [16] are

$$\Delta\beta_{\mp} = \pm\frac{\langle|u_{\ell m}|^2\rangle\ \Omega_\Delta}{\Omega_+ - \Omega_-}\ \left(\frac{\lambda(\ell-1)(\ell+2)}{2k_{\rm eff}R_0}\right)^2\ .$$

Quantitatively, however, the corrections turn out to be negligible, as a quick, order-of-magnitude estimate by using the values of λ and $k_{\rm eff}$ quoted above and $R_0 = 20\ \mu$m shows. But, the corrections to the expressions obtained in Ref. [17] become significant quantitatively, as we will show numerically in the following.

Based on the above discussion, we now present a systematic numerical analysis of the analytical results given in the previous section. The analysis itself is obviously straightforward, but it brings out some numerical consequences that are very relevant to experimental studies of the dynamics of vesicle shape fluctuations. We first analyze two cases, where two important parameters take on different numerical values: case a) $k_{\rm eff} = 100$ erg/cm^2, $b = 10^7$ erg $\cdot$ sec/cm^4, and case b) $k_{\rm eff} = 30$ erg/cm^2, and $b = 2\times10^8$ erg $\cdot$ sec/cm^4, whereas the other parameters assume the same values in both cases (see the captions for the tables and figures). Table 1 together with Figure 1, and Table 2 together with Figure 2 illustrate the numerical results, corresponding to case a) and case b), respectively.

As the numerical results clearly show, case a) and case b) yield two rather different scenarios for the relaxation dynamics of shape fluctuations of quasi-spherical vesicles. In case a), where the values of $k_{\rm eff}$ and b are chosen to conform to the values quoted canonically in the literature, the time scales characterizing the two modes are separated by almost two orders of magnitude, and the slower mode takes up almost all of the full amplitude. Given the typical temporal resolution of milliseconds and the typical accuracy of 10% in determining fluctuation amplitudes in standard flicker-noise analysis experiments [34], only the slower mode can be effectively resolved by experimental observations and analysis. The different physical nature of the two modes are also illustrated by Figure 1. The dispersion relation describing the slower mode is well approximated by $\Omega_{\rm a}(l)$, whereas that describing the faster mode is well approximated by $\Omega_\Delta(l)$. The functional form of $\Omega_{\rm a}(l)$ is the same as that of the dispersion relation derived by Milner and Safran for the relaxation of a pure bending mode in the absence of the coupling between membrane geometry and monolayer density fields [7]. The consequence of the coupling is, however, present in our result. It is indicated by the fact that the bending rigidity appearing in $\Omega_{\rm a}(l)$ is the apparent one, $\kappa_{\rm a}$, which is the result of renormalization of $\kappa_{\rm eff}$ by fluctuations in the monolayer density fields in the presence of the coupling. The reason for the renormalization effect is also revealed in Fig. 1: Fluctuations in the difference of the monolayer density fields relax much more quickly than pure shape fluctuations, i.e. $\Omega_\Delta(l) \gg \Omega_{\rm c}(l)$.

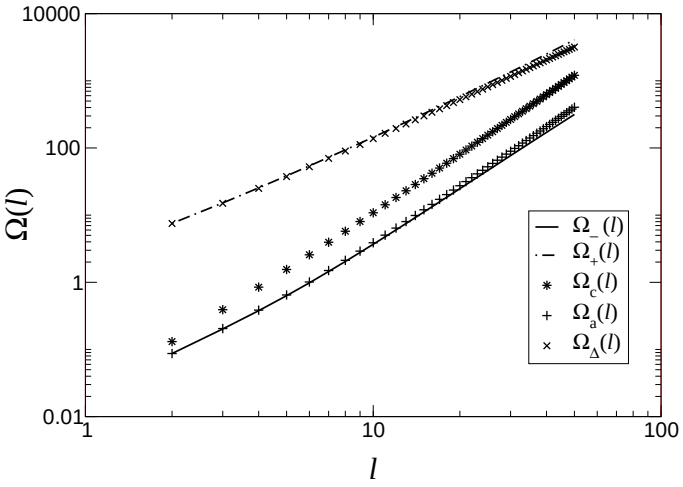

Fig. 1. Various dispersion relations relevant for describing the two dissipative modes of vesicle dynamics for $\kappa_{\rm a} = 10^{-12}$ erg $= 24k_BT$, $\eta = 0.01\,$erg s/ cm^3, $\lambda = 2\times10^{-5}$ erg/ cm, $\Sigma = 10$, $R = 20\,\mu$m, $k_{\rm eff} = 100$ erg/ cm^2, and $b = 10^7$ erg s/ cm^4.

In case b), the quantitative differences between the two relaxation time scales are smaller than in case a), and the slower mode takes up a much smaller fraction of the full amplitude. Relevant to experimental studies is that, for the first few low ℓ values, both relaxation modes can be resolved with the typical experimental resolutions. Another point to note is that there is a reversal in the physical nature of the two modes in comparison with case a), as illustrated by Figure 2. It is now the faster mode that describes approximately the relaxation of bending deformation, where the governing bending rigidity is, however, $\kappa_{\rm eff}$ instead of $\kappa_{\rm a}$. In other words, the renormalization effect is absent. This absence can also easily be rationalized: The relaxations of fluctuations in the difference of the monolayer density fields require longer time scales than the relaxations of pure shape fluctuations. The slower mode no longer describes relaxation of bending fluctuations, although it can not be approximated simply by $\Omega_\Delta(l)$ either. Clearly, case b) provides a new scenario that is different from the "conventional" scenario depicted in case a). Indeed, a recent analysis of data obtained from flicker-noise measurements of giant quasi-spherical vesicles made of stearoyl-oleoyl-phosphatidylcholine [18], which seemed to have resolved two modes with corresponding time scales quantitatively similar to those quoted in Table 2, suggests reasons for searching for this scenario.

We have in the above discussed our interpretation of the monolayer compressibility modulus, $k_{\rm eff}$, and proposed that the values of this parameter should be lower than the standard values quoted in the literature. The numerical analysis illustrates clearly possible consequences that a reduction in the value of $k_{\rm eff}$ can have. As a case of comparison with case b) (Fig. 2) Figure 3 displays the various dispersion relations obtained when the value of $k_{\rm eff}$ is increased to 100 erg/ cm^2 and all the rest of the parameters have the same values as in case b). Quantitatively,

ℓ	2	3	4	5	6	7	8	9	10
τ_-[ms]	11525	4940	2648	1583	1018	691	490	359	271
τ_+[ms]	132	66	39	26	19	14	11	9	7
β_-	0.994	0.987	0.981	0.976	0.970	0.965	0.960	0.954	0.949

Table 1. Numerical values of the time scales, $\tau_\mp \equiv 1/\Omega_\mp$, and the amplitude β_-, characterizing the two dissipative modes of vesicle dynamics for $\kappa_\mathrm{a} = 10^{-12}$ erg $= 24k_BT$, $\eta = 0.01\,\mathrm{erg\,s/\,cm^3}$, $\lambda = 2\times10^{-5}$ erg/ cm, $\Sigma = 10$, $R = 20\ \mu$m, $k_\mathrm{eff} = 100$ erg/ cm^2, and $b = 10^7$ erg s/ cm^4.

ℓ	2	3	4	5	6	7	8	9	10
τ_-[ms]	31977	21796	15485	11378	8625	6720	5362	4366	3617
τ_+[ms]	3185	995	448	241	146	95	65	47	35
β_-	0.287	0.187	0.143	0.117	0.099	0.087	0.077	0.069	0.062

Table 2. Numerical values of the time scales, $\tau_\mp \equiv 1/\Omega_\mp$, and the amplitude β_-, characterizing the two dissipative modes of vesicle dynamics for $\kappa_\mathrm{a} = 10^{-12}$ erg $= 24k_BT$, $\eta = 0.01\,\mathrm{erg\,s/\,cm^3}$, $\lambda = 2\times10^{-5}$ erg/ cm, $\Sigma = 10$, $R_0 = 20\ \mu$m, $k_\mathrm{eff} = 30$ erg/ cm^2, and $b = 2\times10^8$ erg s/ cm^4.

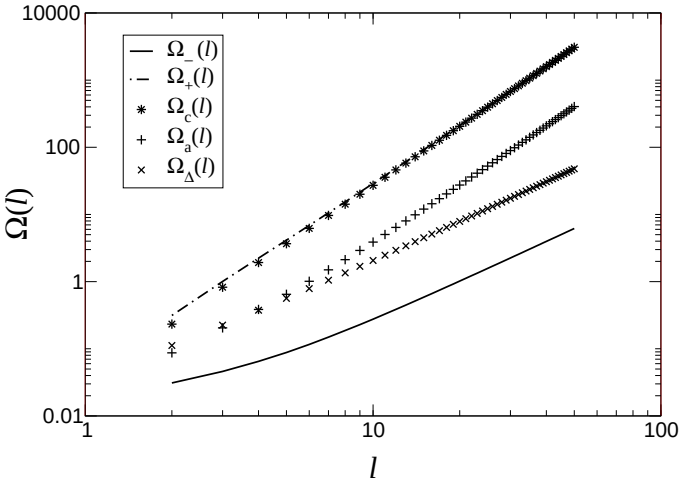

Fig. 2. The same dispersion relations as those illustrated in Fig. 1, for the same parameter values but the following two: $k_\mathrm{eff} = 30$ erg/ cm^2, and $b = 2\times10^8$ erg s/ cm^4.

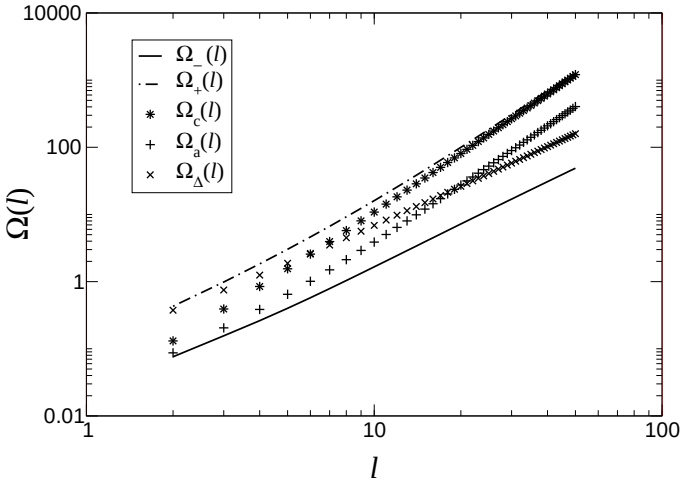

Fig. 3. The same dispersion relations as those illustrated in Fig. 2, for the same parameter values but one: $k_\mathrm{eff} = 100$ erg/ cm^2.

the increase in the value of k_eff reduces the characteristic time scales of both of the modes, affecting the slower mode more significantly, though. There is also a qualitative change in the nature of the two modes for the first few low ℓ values. For the higher value of k_eff, the slower mode reflects predominantly the relaxation of bending deformation governed by the renormalized bending rigidity κ_a, and the faster mode reflects largely the relaxation of the monolayer density-difference field, in reversal to case b). This point serves to underline the need to resolve quantitatively the issue of whether the renormalization by fluctuations of compressibility moduli of lipid-bilayer membranes in systems of giant vesicles is significant enough to be experimentally relevant. To be sure, reductions in the value of k_eff do not always cause the kind of quantitative as well qualitative changes in the relaxation dynamics just discussed. In cases where the intermonolayer friction coefficient, b, has lower values, e.g., $b = 10^7$ erg s/ cm^4, the changes in the relaxation dynamics of the two modes for low ℓ values are not significant for the same increase in the value of k_eff.

Another point to discuss in connection with experimental studies of vesicle fluctuations by the technique of flicker-noise measurement and analysis concerns the effects that variations in the parameter Σ have on the relaxation dynamics of the fluctuations, as Σ is a vesicle-specific parameter that typically varies in the range from 0 to 25 [34]. We have checked systematically in the numerical analysis the effects, which are summarized by a comparison of Figure 4 with Figure 2. It is easy to see that a reduction in Σ from 10 to 0 leads to a significant increase in the characteristic time scale of the slower mode, but very small increase in the time scale characterizing the faster mode. Moreover, the relative positions of the different dispersion relations do not change qualitatively.

For the sake of completeness of the discussion on the dissipative dynamics, we mention an analytical relationship between $\Omega_-(\ell)$ and $\Omega_+(\ell)$, which may be exploited

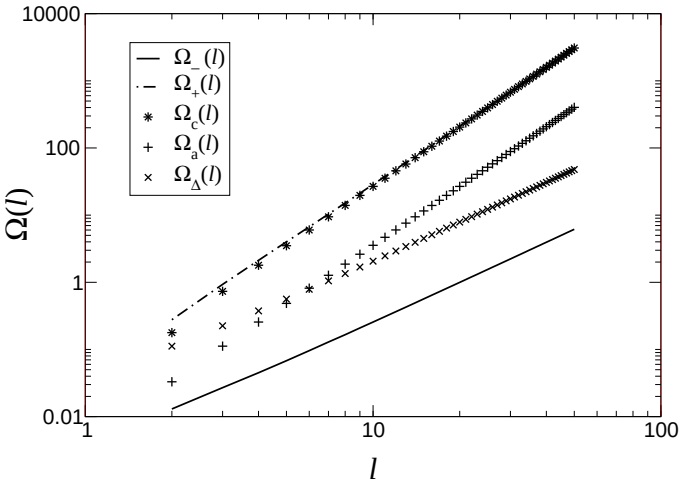

Fig. 4. The same dispersion relations as those illustrated in Fig. 2, for the same parameter values but one: $\Sigma = 0$.

in analysis of experimental data. This relationship and its potential have already been pointed out independently in Ref. [18]. It follows straightforwardly from Eq.(89) that

$$\begin{aligned} \Omega_-(\ell)\ \Omega_+(\ell) &= \Omega_{\rm a}(\ell)\ \Omega_\Delta(\ell) \\ &= \frac{\ell(\ell+1)(\ell-1)(\ell+2)\ \kappa_{\rm a}}{\eta R_0^3 \Gamma_\ell}\left[\ell(\ell+1)+\Sigma\right] \\ &\quad \cdot \frac{\ell(\ell+1)}{2R_0^2}\ \left(\frac{k_{\rm eff}}{b}\right)\ . \end{aligned} \tag{100}$$

In the above expression, all quantities may be considered known except the ratio $k_{\rm eff}/b$. Thus, for vesicle systems where the two relaxation processes can both be resolved experimentally, the product $\Omega_-(\ell)\ \Omega_+(\ell)$, and in turn, $k_{\rm eff}/b$, can be quantitatively determined. This quantitative information may be used to obtain a quantitative measure of the intermonolayer friction coefficient b, provided that $k_{\rm eff}$ can be obtained by use of other independent methods, e.g. the micromechanical technique [25]. This method of determining b can serve both as an alternative to, and a check of, the method used previously for estimating the value of b [14].

Finally, we now return to the issue of the validity of the no-inertia approximation, which has already been mentioned in Section 4. This discussion is relevant, especially in view of the recent publication of Pott and Méléard [18], in which the experimental data seems to suggest that the dynamics of quasi-spherical vesicles is not purely dissipative, but that the relaxation is modulated by an oscillatory component of a small, but observable amplitude. Recapitulating Eq. (45), and using $\rho_{\rm b} = 1$ g/cm^3 and $\eta = 0.01$ erg $\cdot$ sec/cm^3 for water, we have

$$\bar{\mathcal{R}} = 10^{-6}\frac{\alpha^2}{t_0}\ .$$

Setting $\alpha = 60$ which corresponds to the lowest spherical harmonic mode, and using the shortest time scales given in Table 1 and Table 2, for the two different cases a) and b), respectively, we get two corresponding quantitative estimates, $\bar{\mathcal{R}} \simeq 0.04$ and $\bar{\mathcal{R}} \simeq 0.001$. The issue is then really whether these numbers can be effectively treated as zero. A theoretical analysis that may address this issue clearly must take into account the inertial term in the bulk hydrodynamics and is outside the scope of this paper. But, if the approximation turns out to be valid, then the theory we have presented here does not provide an explanation for the observed oscillatory behaviour. One may indeed question whether the observed oscillatory behaviour is genuine. If, however, the oscillatory behaviour is genuine, then the no-inertia approximation should be re-examined by studying the effect of the inertial term on the vesicle dynamics . Moreover, one needs to bear in mind that, if it is indeed the inertial term that is responsible for the oscillatory behaviour, the time scales that characterize the part of the exponential relaxation of the dynamics should in principle be qualitatively different from the times scales obtained from a theory of purely dissipative dynamics such as the one presented in this paper. Looked at from this point of view, the interpretation given by the authors of Ref. [18] of their experimental data, which was based on their earlier theory of purely dissipative dynamics [17], does not appear consistent with the same data which shows the presence of an oscillation.

For the dynamics of the density-sum field, whose purely dissipative dynamics would be characterized by a time scale of the order of 10^{-7} seconds, it is certain that the no-inertia approximation does not hold. Consequently, the dynamics of this field will contain an oscillatory component. We may argue, however, that this dynamics will have no observable effect on the dynamics of the other two modes. One argument is that the coupling of the density-sum field to the other two fields implied by the free energy is very weak for giant vesicles (and is in fact non-existent for planar membranes, at least within the framework of linearized theories). Another argument is that the time scales associated with the relaxation-oscillation dynamics of the density-sum field would still be very short compared to the time scales characterizing the dynamics of the other two fields.

We would like to end this paper by stating our two main hopes that come with the presentation of the work. First, the current theoretical work will encourage more systematic and careful experimental work that will lead to a clear and quantitative understanding of the dynamics of vesicle shape fluctuations; second, the fact that the theory is built upon certain fundamental principles and considerations, together with the systematic nature of its formulation, will be exploited in terms of extensions of the theory that will describe vesicle systems formed of fluid bilayers containing more than one molecular species (e.g. a second lipid or a protein).

Aknowledgement
LM and ML acknowledge the financial support from University of Southern Denmark in the form of a research grant and in the form of a Ph.D. fellowship. The authors are grateful to Per Lyngs Hansen, John Hjort Ipsen, Jonas Henriksen and Ole G. Mouritsen for helpful discussions and critical reading of the manuscript. The MEMPHYS Center for Biomembrane Physics is supported by the Danish National Research Foundation.

A Appendix

In this Appendix, we will sketch briefly the calculations of static correlation functions based on the free-energy model, Eq.(12). Eq.(12) can be expressed in a form more convenient for the calculations presented here:

$$\hat{F} = \int d\hat{A} \left\{ k_{\rm eff}(\hat{\phi}^{\Delta})^2 + k_{\rm eff}(\hat{\phi}^{\Sigma})^2 + 2\kappa_{\rm eff}\hat{H}^2 + 2\lambda\hat{H}\hat{\phi}^{\Delta} + \sigma_0 \right\} , \tag{101}$$

where the use of the "hat" over the variables indicates that they should be considered as stochastic variables.

The calculations of the static correlation functions are essentially based on a Gaussian theory of the fluctuations. An inevitable issue in the calculations concerns the choice of an appropriate set of *independent* degrees of freedom, whose fluctuations must be integrated over. Although $\hat{u}_{\ell m}$, $\hat{\psi}^{\Delta}_{\ell m}$ and $\hat{\psi}^{\Sigma}_{\ell m}$, as defined in Eqs.(40)-(42), respectively, are independent of each other and appear directly in the free-energy expression, they are not appropriate in general. To make the point clear, consider a local area element of membrane surface, A_{Δ}, associated with which are N^{+}_{Δ} and N^{-}_{Δ} lipid molecules in the outer and inner monolayer, respectively. Changes in the local monolayer density fields, ϕ^{Δ} and ϕ^{Σ} can then be brought about by two types of independent physical processes: lateral flows of lipid molecules at fixed surface geometry, which lead to changes in N^{+}_{Δ} and N^{-}_{Δ} at fixed A_{Δ}; and, a change in the surface geometry at fixed N^{+}_{Δ} and N^{-}_{Δ}, which changes A_{Δ}. Thus, it is more meaningful to choose, together with the $u-$field, the fluctuating fields that reflect the former process, as the appropriate set of independent degrees of freedom. Such fields, denoted henceforth by $\hat{n}^{\pm}(\theta,\varphi)$, are related to the apparent density fields as follows:

$$\begin{aligned}\hat{\rho}^{\pm}(\theta,\varphi) &\equiv [\rho^{\pm}_0 + \rho_0\hat{n}^{\pm}(\theta,\varphi)]\frac{1}{\sqrt{g(\hat{u})}} \\ &= [\rho^{\pm}_0 + \rho_0\hat{n}^{\pm}(\theta,\varphi)][1+g_2(\hat{u})] ,\end{aligned} \tag{102}$$

where $g(\hat{u}) \equiv a(\hat{u})/R_0^2$ and $g_2(\hat{u}) \equiv -2\hat{u}+3\hat{u}^2-(\boldsymbol{\nabla}_{\rm L}\hat{u})^2/2$ is the expansion of $1/\sqrt{g(\hat{u})}-1$ up to second order in $\hat{u}$. It follows easily that

$$\begin{aligned}\hat{\phi}^{\Delta}(\theta,\varphi) &= \phi^{\Delta}_0 + \hat{n}^{\Delta}(\theta,\varphi) + \phi^{\Delta}_0 g_2(\hat{u}) + \hat{n}^{\Delta}(\theta,\varphi)g_2(\hat{u}) \\ \hat{\phi}^{\Sigma}(\theta,\varphi) &= \hat{n}^{\Sigma}(\theta,\varphi) + g_2(\hat{u}) + \hat{n}^{\Sigma}(\theta,\varphi)g_2(\hat{u}) ,\end{aligned} \tag{103}$$

where $\hat{n}^{\Delta}(\theta,\varphi) \equiv (\hat{n}^{+}(\theta,\varphi)-\hat{n}^{-}(\theta,\varphi))/2$ and $\hat{n}^{\Sigma}(\theta,\varphi) \equiv (\hat{n}^{+}(\theta,\varphi)+\hat{n}^{-}(\theta,\varphi))/2$.

Expanding the free energy given in Eq.(101) to second order in the fluctuations degrees of freedom, eliminating $\hat{u}_{00}$, $\hat{n}^{\Sigma}_{00}$ and $\hat{n}^{\Delta}_{00}$ using the fixed-volume and the fixed-molecular number constraints

$$\hat{u}_{00} = -\frac{1}{\sqrt{4\pi}}\sum_{l\geq 1}\sum_{m=-l}^{l}|\hat{u}_{\ell m}| , \tag{104}$$

$$\hat{n}^{\Delta}_{00} = \text{Const.} , \tag{105}$$

$$\hat{n}^{\Sigma}_{00} = \text{Const.} , \tag{106}$$

leads to the following expression:

$$\begin{aligned}\hat{F} = \text{Const.} \\ + \sum_{\ell,m}{}' \Big\{ \frac{1}{2} \big\{ (\ell-1)(\ell+2)[\ell(\ell+1)\kappa_{\rm eff} + \sigma_0 R_0^2 \\ -\kappa_{\rm s}(\phi_0^{\Delta})^2 + 4\lambda R_0 \phi_0^{\Delta}] + 8\kappa_{\rm s}[1+(\phi_0^{\Delta})^2] \big\} \, |\hat{u}_{\ell m}|^2 \\ +\kappa_{\rm s}\,(\hat{n}^{\Delta}_{\ell m})^2 + \kappa_{\rm s}\,(\hat{n}^{\Sigma}_{\ell m})^2 - [(\ell-1)(\ell+2)\lambda R_0 \\ +4\kappa_{\rm s}\phi_0^{\Delta}]\;\hat{u}^*_{\ell m}\hat{n}^{\Delta}_{\ell m} - 4\kappa_{\rm s}\;\hat{u}^*_{\ell m}\hat{n}^{\Sigma}_{\ell m} \Big\} , \qquad (107)\end{aligned}$$

where $\kappa_{\rm s} \equiv k_{\rm eff} R_0^2$.

Based on the above Gaussian theory for the fluctuations, and noting that, to the first order in fluctuations,

$$\hat{\psi}^{\Delta}_{\ell m} = \hat{n}^{\Delta}_{\ell m} - 2\phi_0^{\Delta}\hat{u}_{\ell m} \, , \qquad (108)$$

we finally obtain the following two static correlation functions, [4]

$$\langle |\hat{u}_{\ell m}|^2 \rangle = \frac{k_{\rm B}T}{(\ell-1)(\ell+2)\kappa_{\rm a}[\ell(\ell+1)+\Sigma]} \, , \qquad (109)$$

which has been quoted in Eq.(97) and Eq.(98), and

$$\langle \hat{u}^*_{\ell m}\hat{\psi}^{\Delta}_{\ell m} \rangle = \frac{(\ell-1)(\ell+2)\lambda R_0}{2\kappa_{\rm s}} \langle |\hat{u}_{\ell m}|^2 \rangle \, . \qquad (110)$$

[4] Other correlation functions can be obtained just as straightforwardly, but they are not listed here.

References

1. F. Brochard, J. F. Lennon, J. Phys. France **36** 1035 (1975).
2. W. Helfrich, Z. Naturforsch. **28c** 693 (1973).
3. Useful reviews on the subject are U. Seifert, R. Lipowsky, in Vol. 1 of *Structure and Dynamics of Membranes*, edited by R. Lipwosky and E. Sackmann (Elsevier, Amsterdam, 1995), and U. Seifert, Adv. Phys. **46** 13 (1997).
4. K. Berndl, J. Käs, R. Lipowsky, E. Sackmann, U. Seifert, Europhys. Lett. **13** 659 (1990).
5. L. Miao, U. Seifert, M. Wortis, H. G. Döbereiner, Phys. Rev. E **49** 5389 (1994).
6. H.-G. Döbereiner, E. Evans, M. Kraus, U. Seifert, M. Wortis, Phys. Rev. E **55** 4458 (1997).
7. S. T. Milner, S. A. Safran, Phys. Rev. A **36**, 4371 (1987).
8. J. F. Faucon, M. D. Mitov, P. Méléard, I. Bivas, P. Bothorel, J. Phys. (France) **50** 2389 (1989).
9. M. D. Mitov, J. F. Faucon, P. Méléard, P. Bothorel, in *Advances in Supermolecular Chemistry* Vol. 2, edited by G. W. Gokel (JAI Press Inc., Greenwich, 1992), pp.93-139.
10. M. B. Schneider, J. T. Jenkins, W. W. Webb, J. Phys. France **45** 1457 (1984).
11. U. Seifert, L. Miao, H. G. Döbereiner, M. Wortis, in *The Structure and Conformation of Amphiphilic Membranes*, Vol. 66 of *Springer Proceedings in Physics*, edited by R. Lipowsky, D. Richter, K. Kremer (Springer, Berlin, 1992), pp.93-96.
12. W. Wiese,, W. Harbich, W. Helfrich, J. Phys. Condensed Matter **4** 1647 (1992).
13. R. Waugh, J. Song, S. Svetina, B. Žekš, Biophys. J. **61** 974 (1992).
14. E. Evans, A. Yeung, R. Waugh, J. Song, in *The Structure and Conformation of Amphiphilic Membranes*, Vol. 66 of *Springer Proceedings in Physics*, edited by R. Lipowsky, D. Richter, K. Kremer (Springer, Berlin, 1992), pp. 146-153.
15. U. Seifert, S. A. Langer, Europhys. Lett. **23** 71 (1993).
16. A. Yeung, E. Evans, J. Phys. II France **5** 1501 (1995).
17. I. Bivas, P. Méléard, I. Mircheva, P. Bothorel, Colloids Surf. A **157** 21 (1999).
18. T. Pott, P. Méléard, Europhys. Lett. **59** 87 (2002).
19. L. Onsager, Phys. Rev. **37** 405 (1931); Phys. Rev. **38** 2265 (1931).
20. U. Seifert, Adv. Phys. **46** 13 (1997).
21. P. L. Hansen, L. Miao, J. H. Ipsen, Phys. Rev. E **58** 2311 (1998).
22. W. Cai, T. C. Lubensky, Phys. Rev. E **52** 4251 (1995).
23. J.-B. Fournier, A. Ajdari, L. Peliti, Phys. Rev. Lett. **86** 4970 (2001).
24. F. David, S. Leibler, J. Phys. II (France) **1** 959 (1991).
25. E. Evans, W. Rawicz, Phys. Rev. Lett. **64** 2094 (1990).
26. R. Aris, *Vectors, Tensors and basic Equations of Fluid Mechanics* (Dover Publications Inc., New York, 1962).
27. J. T. Jenkins, J. Math. Biology **4** 149 (1977).
28. L. D. Landau, E. M. Lifshitz, *Fluid Mechanics*, second edition (Butterworth-Heinemann, 1998).
29. S. Kim, S. J. Karrila, *Microhydrodynamics: Principles and Selected Applications* (Butterworth-Heinemann, 1991).
30. U. Seifert, Eur. Phys. J. B **8**, 405 (1999).
31. L. E. Reichl, *A Modern Course in Statistical Physics* (University of Texas Press, Austin, 1980).
32. W. Helfrich, J. Phys. (Paris) **46** 1263 (1985); L. Peliti, S. Leibler, Phys. Rev. Lett. **54** 1690 (1985); H. Kleinert, Phys. Lett. **114A** 263 (1986).

33. B. W. Koenig, H. H. Strey, K. Gawrisch, Biophys. J. **73** 1954 (1997).
34. J. R. Henriksen, *A Theoretical and Experimental Investigation of the Mechanical Properties of Giant Unilamellar Vesicles* (Master Thesis, Technical University of Denmark, 2000).